The Role of the Thermal Contact Conductance in the Interpretation of Laser Flash Data in Fiber-Reinforced Composites

by

Carlos Mariano Alvarado

Thesis submitted to the Faculty of the
Virginia Polytechnic Institute and State University
in partial fulfillment of the requirements for the degree of

MASTER OF SCIENCE
in
Mechanical Engineering

APPROVED:

James R. Thomas, Ph.D., Chairman

Brian Vick, Ph.D.

D.P.H. Hasselman, Ph.D.

April, 1993
Blacksburg, Virginia

The Role of the Thermal Contact Conductance in the Interpretation of Laser Flash Data in Fiber-Reinforced Composites

by

Carlos Mariano Alvarado
Dr. James R. Thomas, Chairman
Mechanical Engineering

(ABSTRACT)

The flash method proposed by Parker et al. in the early sixties is one of the most important experimental procedures to determine the thermal properties of homogeneous materials. Because of the versatility of this method, researchers have attempted to extend its usefulness into the realm of composite material. However, some difficulties arise because of the existence of preferential heat paths in heterogeneous materials, especially in fiber-reinforced composites. In order for experimental flash method results to be meaningful a homogeneous temperature front must exist at the back face of the sample, where the measurements are made.

In this work, the parameters that render the radial temperature response of a fiber-reinforced composite homogeneous at the back face were investigated. According to the literature three criteria must be met for homogeneity to occur: fiber-to-matrix volume ratio must be high; sample axial dimension must be large compared to radial fiber dimension; and the thermal contact between the fibers and the matrix must be high. Since the first two criteria are met by most fiber-reinforced composite samples subject to the flash method, attention was concentrated on the third criterion. An inequality that must be met by the contact conductance term to establish homogeneity is proposed and some sample temperature profiles are presented.

ACKNOWLEDGMENTS

Foremost, I would like to express my gratitude to fellow high end audio enthusiast and music lover, Dr. J. R. Thomas. He more than fulfilled his role as principal thesis advisor. Dr. Thomas was always enthusiastic, always ready to help, and always willing to offer his insightful suggestions, even when the research seemed to be going nowhere. More important than this, he never hesitated to do all he could to make sure I got the financial support I needed to get through this past academic year. I am most thankful for all your help and guidance.

To the members of my graduate committee, Dr. D.P.H. Hasselman and Dr. B. Vick, I thank you for the advise and assistance that was always there when needed.

To Dr. C. H. Stern, the instructor who first introduced me to field of heat transfer, I thank you for helping me to develop a deep appreciation for thermodynamics and heat transfer. The classes I took under you became exciting journeys into the unknown, which ultimately motivated me to attend graduate school.

I gratefully acknowledge the Mechanical Engineering department at VPI and the U.S. Department of Energy and for their financial assistance and support.

There are no words that can adequately express the feelings of gratitude I have for my parents. Without you none of this would have been possible. I thank you for giving me the encouragement and inspiration to do my best during my years at VPI. Your emotional support has been invaluable. Again, thank you for everything.

TABLE OF CONTENTS

LIST OF FIGURES

CHAPTER 1

1.1 Introduction

A composite material is one that results when two or more materials, each having its own different characteristics, are combined to produce a new one with improved properties for specific applications. Each input material should serve a specific function in the composite, which in turn should show distinctive new or improved properties [1]. For example, to make concrete effective in handling loads in tension as well as loads in compression (concrete's most effective application) it is customary to insert rods of steel into the cement mixture. This new material, which is a composite, can then be used in structures that must support bending (simultaneous tension & compression) loads more effectively.

Advanced composites posses enhanced rigidity and lower density compared to conventional materials. These materials comprise structural materials developed for high technology applications, such as airframe structures, for which other materials are not sufficiently firm. In these materials extremely stiff and strong continuous or discontinuous fibers, whiskers or small particles are dispersed in the matrix. Most common matrix materials include ceramics, glasses, metals, and polymers [1].

There is a growing awareness in the United States that, to maintain a competitive edge, new materials must be developed and exploited. Because of this the use of fiber-reinforced materials in engineering applications has grown rapidly. Selection of a

composite rather than a monolithic material for a given application is dictated by its properties. Frequently, the high values of stiffness and strength will be the deciding factors. In other applications, the selection of a composite material reflects the unique properties of the matrix in combination with the reinforcing fibers, for example, advanced composites that exhibit wear resistance or undiminished strength at very high temperatures [1].

The first applications for advanced composite materials were in aerospace structures and in sports equipment. Recently applications have included artificial joints and organs, reinforced building materials, automotive components, marine structures and high end audio equipment [1]. Below is a brief sample of how composites are being used in these different fields.

Aerospace: Advanced organic-matrix fiber-reinforced composites are used extensively on commercial production aircraft manufactured by such companies as Boeing and Airbus. Advanced carbon-reinforced composites have also found wide acceptance in military aerospace applications. A good example of composites in this field is the use of brake materials consisting of carbon fibers embedded in a carbonaceous matrix. These carbon-carbon composites offer low weight, excellent friction behavior and wear resistance [1].

Automotive: The need to build lighter, quieter, and more fuel efficient engines has motivated the use of composites in this field. An example is the use of a metal matrix composite to selectively reinforce the crown and ring groove in diesel engine pistons to improve thermal fatigue and wear [1].

Sporting products: Used in the frames of rackets for tennis are boron fiber- or carbon fiber-reinforced epoxies. Another example is golf club shafts which use hot forged Al-SiC whisker composite for added rigidity and control. High-performance sailing crafts fabricated from carbon fiber-reinforced plastics have strong, stiff, lightweight hulls.

Bicycle frames fabricated from boron-aluminum composite, and rims fabricated from an aluminum-aluminum oxide composite are stronger and lighter than those made by conventional materials [1].

Electronics: Conventional heat sinks used to remove heat from integrated circuits have a coefficient of thermal expansion different from that of the circuit thus leading to the failure of the device by thermal fatigue. However, heat sinks fabricated from metal matrix composites with matched properties have done away with this problem [1].

This last example shows why investigators have devoted a great deal of effort to the understanding of thermal properties of composite materials. The knowledge of thermophysical properties for these new materials is essential for their analysis in severe environments with thermal gradients. Below are summarized three important aspects of this type of research that are relevant to the present study:

1. Theoretical and computational analysis of the heat equation in composite materials
2. Theoretical evaluation of transport properties of composite materials
3. Experimental evaluation of transport properties of composite materials

Theoretical and computational analysis of the heat equation

Carslaw and Jaeger [2] summarized in their classic textbook much of the most important studies done in this area before the mid 50's. In this work they used complex variable and residue theory to obtain temperature distributions. This method is effective for two-layered composites, but becomes intractable if the number of layers increase. Vodicka [3,4] offered the first significant contribution to solving problems of this type in two papers published in 1950 and 1955. A feature in these solutions was a new type of orthogonality relation along with the very well known method of separation of variables. Bulavin and Kascheev [5] used this method in 1965 to solve the heat equation in a composite with an arbitrary number of layers under rather restrictive boundary conditions.

In 1967, Beach [6] investigated heat transfer in multi-layer cylinders with perfect thermal contact, while Moore [7] found the temperature distribution in a two-layer slab allowing for contact resistance between the layers.

In 1972 Mulholland and Cobble [8] developed a novel method to find the temperature distribution in a composite using fairly general boundary conditions. These researchers allowed for arbitrary initial conditions within each of the different layers and for heat exchange at the external boundaries. They obtained the solution by transforming the original differential equation to one with homogeneous external boundary conditions, and solved it using the Vodicka orthogonality relation. This solution yielded the temperature distribution in each of the layers at any time and location under the most general type of linear boundary and initial conditions. Even though this study allowed for considerable generality, it required the different layers of the composite to be isotropic.

In 1975 Padovan [9] addressed this limitation and developed transient solutions for semi-infinite *anisotropic* laminated slabs and cylinders. This worker transformed the governing heat equation into a complex version of the Vodicka-Tittle problem using the conjugate properties of the set. This study is rather advanced and abstract. Another aspect of heat conduction in composites that had not received very much attention was the effect of thermal resistance in the interface of different materials. Baker-Jarvis and Inguva [10] in 1985 focused on this parameter and developed a general theoretical framework. This solution considered multidimensional, non-homogeneous problems with specified contact resistance. This solution followed using a quasi orthogonal eigenfunction expansion and Green's functions. Yet another neglected parameter was given due attention in 1991 when Choi and Thangjitham [11] presented a study that considered the role of flaws in composite materials such as cracks or debondings. The key for this solution was the use of a flexibility matrix to formulate the boundary value problem for the

multi-layer medium and the application of Chebyshev polynomials to the resulting integral equation.

A very interesting paper appeared in 1987, after some recent experimental results had suggested the existence of thermal waves at the interface of different materials. Frankel, Vick and Ozisik [12] developed a theoretical justification for this odd phenomenon modifying Fourier's law to include a thermal relaxation time. Thus, transformed was the familiar parabolic heat equation into a more general hyperbolic partial differential equation. A generalized finite integral transform technique was proposed in the flux domain and a general solution was developed. This paper is a good example of how sophisticated the analysis of heat conduction in composite materials has become.

Some other mathematical techniques have been offered by different authors to analyze heat conduction in composite materials. For example in 1988 Haji-Sheikh [13] proposed a new method by constructing basis functions that preserve the continuity of temperature (thus assuming perfect thermal contact) and flux throughout the domain and boundaries of the composite. These functions can then be used in conjunction with Green's functions and through the Galerkin method a solution can be obtained. Other authors have focused their attention on theoretical models that attempt to improve certain thermal properties of composites. For example in 1992 Gordaninejad [14] demonstrated that the thermal conductivity of polymeric-fiber reinforced composites can be improved by using coated fibers and by adding thermally conducting micro-spheres to the resin. Two- and three-dimensional finite element unit cell models were developed to predict the directional thermal conductivity.

Some authors believe that even though analytic expressions are elegant and relatively simple to evaluate they have a rather restrictive range of applicability. In 1986 James, Wostenholm, Keen, and McIvor [15] obtained a very general solution to the two-dimensional, steady-state problem using the finite difference technique. These researchers

feel that a very rigorous solution can be obtain with this method but admit that it requires extensive calculation. They used this solution to study the effect of heat flow in anisotropic materials.

Theoretical evaluation of transport properties of composite materials

In 1973 Horvay, Mani, Veluswami and Zinsmeister [16] developed a solution to the problem of determining the temperature distribution in a semi-infinite laminated composite subject to time-harmonic boundary excitation. The matrix and fiber were in perfect thermal contact, and stacked parallel to the heat flow direction. Effective thermal properties were proposed from this solution. Han and Cosner [17] published a study in 1981 on the effective thermal conductivity of fibrous composites having isotropic fibers dispersed in an isotropic matrix under *transverse* heat flow and steady-state conditions. One of the more important observations in this study was that the effect of the effective thermal conductivity ratio was governed by the distance between two adjacent fibers measured along the heat path direction.

A very advanced and general study was done by Beneveniste and Miloh [18] to find the effective thermal conductivity of composite media in which a thermal resistance exists at the interfaces. They applied the principles of defining and computing effective moduli and generalized them to include the thermal barrier term. This procedure was applied to derive the effective conductivity of a composite with embedded spherical inclusions at a *dilute* concentration.

Hasselman and Johnson [19], however take a more clever approach and re-derived the results proposed by Maxwell and Rayleigh last century to include an interfacial thermal resistance term. The derived effective conductivity term applies to a composite consisting of a matrix embedded with small concentrations of dispersions. A direct consequence of

this result is that the effective conductivity not only depends on volume fractions, but also on dispersion dimensions.

In a later study Hasselman [20] conducted experimental analysis to verify the validity of the results presented in [19]. Specifically, this investigator compared experimental data with models based on Bruggeman's variable dispersion theory, which assumes perfect thermal contact, and found very significant discrepancies between theory and experiment. These differences were reconciled when the thermal barrier term was added to the theoretical formulation. He also included a picture of a fiber-reinforced composite showing clear cracks at the interfaces that significantly contribute to thermal resistance, thus authenticating his concerns for this important factor.

Another study by Hasselman et al. [21] considered the thermal diffusivity of a bi-axial SiC composite heated to very high temperatures. This composite was found to exhibit an increase of conductivity parallel to the fiber. The opposite effect was found in a direction perpendicular to the fibers. This decrease was attributed to interfacial debonding and therefore an increase in thermal barrier between the two constituents of the composite. This study provided yet more evidence for the importance of thermal barriers in composite materials.

Experimental evaluation of transport properties of composite materials

One of the most significant studies in this field came in 1961. In a classic paper, Parker, Jenkins, Butler, and Abbott [22] proposed a new method for determining the thermal diffusivity, conductivity and heat capacity by the application of the flash method. Before this research most methods relied on measurements done during steady-state conditions. Accurate data required large samples and lengthy time intervals (especially for poor thermal conductors). In the flash technique a test sample is irradiated uniformly on one side using an energy pulse. The *average* temperature rise of the opposite side is

measured as a function of time, using an infrared detector or thermocouple. The recorded data is fit to a curve, and the diffusivity calculated. Both the test and the data recording can be conducted in a few minutes. A typical sample size for the flash method is about 2 mm thick. This is ideal for high-conductivity materials or those manufactured in thin layers, such as semiconductor substrate wafers. This method has been used to make measurements on materials whose thermal diffusivities range from .001 to 10 cm^2/s. Dimensionless back face time-temperature histories obtained from this method also allow for comparison between experimental results and theoretical models. This is such an effective procedure for determining thermal properties that it is being considered as a standard test method by the American Society for Testing and Materials (ASTM).

Theoretically, the back face temperature response of a homogeneous material subject to flash experiment is given by

$$\frac{T(L,t)}{T_{\max}} = 1 + 2\sum_{n=1}^{\infty}(-1)^n e^{-(n\pi/L)^2 \alpha t}. \qquad (1\text{-}1)$$

Note that this equation assumes that all boundaries are insulated and that the energy pulse is deposited in the sample instantaneously. The thermal diffusivity can be determined from the time it takes the back face temperature to reach half the maximum temperature ($t_{1/2}$). For this condition the infinite series can be approximated by the first term only, and it follows that the thermal diffusivity is given by

$$\alpha = 1.38\frac{L^2}{\pi^2 t_{1/2}}. \qquad (1\text{-}2)$$

Even though this method had originally been proposed to measure the thermal properties of homogeneous materials, its implementation quickly extended into the field of heterogeneous materials. However, since the method is based on the average back face temperature, only "effective" thermal properties can be determined from it. These

effective properties lump in one number all the non-homogeneous effects of the composite material. As discussed previously workers have proposed equations for the effective properties of heterogeneous material based on volume fraction and constituent property as far back as 1892 when Rayleigh and Maxwell suggested one such formula. Their equation assumed dilute dispersions where the average distance between dispersed particle is much larger than particle size. A rigorous solution for the effective thermal conductivity of a random array of particles of arbitrary sizes has not been achieved.

Because of this limitation some investigators have sought to compare experimental values of diffusivity with calculated values and have developed criteria for the level of tolerable heterogeneity. Lee and Taylor [23] published an important work done to address this issue. They studied samples composed of copper embedded in an epoxy matrix, with copper volume ranging from 1.8% to 28.6%. In all cases when the content of the dispersed phase was less than 25%, agreement between theory and experiment was excellent. These results proved that the flash diffusivity method is applicable to heterogeneous materials within certain limits. The method, however, is not as successful in evaluating layered composites if the heat pulse travels parallel to the layers.

In 1985 Taylor, Jortner, and Groot [24] studied the applicability of the flash technique to fiber-reinforced composites. They recognized that while the usefulness of this technique had been demonstrated previously for randomly dispersed composites, problems arise from preferential heat paths in fibrous reinforced composites. After studying a carbon-carbon composite they found that the degree of mismatch between the measured back face temperature and the homogenized theoretical model depended upon three parameters:

1. the relative value of the diffusivities of the fiber and the matrix;
2. the thickness of the sample;
3. the rear face area of sample sensed by the monitor.

When the sample is reasonably thick in the longitudinal direction or when the ratio of diffusivities approaches unity, the response approximates the theoretical model for a homogeneous material. Furthermore, the thermal diffusivity was found to depend on the intervals of time of the back face temperature rise. The diffusivities values calculated at various percent rises decreased with increasing percent rise. For example, the diffusivity calculated at 50% of the back face temperature rise is higher than that calculated at 85% of the rise.

In 1986 Balageas and Luc [25] successfully identified the parameters governing the transient thermal behavior of directional reinforced composites. They also established that the application of the homogeneous model, under certain conditions, is erroneous and that it may lead to significant errors. These researchers found that, using conventional methods, the measured diffusivity of a composite is not constant with respect to time or sample thickness. They found that as the sample thickness becomes large compared to the distance between the fiber and the matrix, the values calculated for the diffusivity approach that of a homogeneous medium. However, this is only true if the thermal contact resistance between the fiber and the matrix is negligible, and if the fiber volume fraction is high. This statement agrees with the conclusions of Taylor, et al. [24]. Balageas and Luc also found that the thermal behavior depended on three important parameters: the volume content of the fiber; the fiber-to-matrix ratio of thermal conductivity and of specific heat, and the contact thermal resistance between the two components. These investigators concluded by stating that traditional techniques, such as the flash method, can be used to study composites, but only along with new interpretations that take into account the real structure of the composite. For mathematical description they suggest using a model in which each phase is homogenized separately, but are coupled together through a contact conductance term.

1.2 Motivation for the Present Work[1]

In general, two methods are available to estimate thermal properties of materials. Those that rely on transient temperature distributions, and those that assume steady-state conditions of heat flow. Transient methods yield values for thermal diffusivity, while steady-state conditions provide values for thermal conductivity. Thermal conductivity and thermal diffusivity are related by the definition:

$$\alpha = \frac{k}{\rho c} \tag{1-3}$$

where α is the thermal diffusivity, k is the thermal conductivity, ρ is the density, and c is the heat capacity. Therefore, if density and heat capacity are known, both steady-state and transient methods furnish all relevant thermal properties.

For the purpose of this work, a composite material is considered to be a heterogeneous material which is composed of two or more homogeneous materials. The different homogeneous components of a composite often have very different thermal properties of their own. This property discontinuity will give rise to preferential heat flow paths in a composite, as discussed by Taylor et al. [24]. This means that equation (1-3) is not generally applicable to this type of material. However, certain conditions under which an effective thermal diffusivity is valid have been discussed above. For example, Taylor et al. [24] has shown that the effective diffusivity concept is sound for a composite made up of a randomly distributed phase as long as the scale of this phase is small with respect to the size of the sample.

However, the type of material of interest for this study is not a composite with a randomly dispersed phase, but a carbon fiber-reinforced polymer matrix composite. This

[1]Several of the ideas presented in this section were taken from reference [26]. A paper which includes the present author as a secondary co-author.

is the family of composites studied by Taylor et al. [24] and Balageas et al. [25]. For simplicity, it is assumed that in these materials, the fibers run continuously in one direction and that the fibers are uniformly distributed within the matrix. Two major modes of heat transfer are possible in these composites: transverse and longitudinal. The transverse mode involves heat flow perpendicular to the fibers.

For transverse heat flow the scale (diameter) of the fibers is much smaller than sample size, therefore the homogeneity criterion established by Taylor et al. [24] is satisfied. Consequently, an effective thermal diffusivity based on heat transfer perpendicular to the fibers is possible. For heat transfer parallel to the fibers, however, the dimension of the fibers is the same as sample dimension. In this case the Taylor criterion is not satisfied, and equation (1-1) does not apply in general. For carbon fiber-polymer matrix composites the fiber-to-matrix thermal conductivity ratio exceeds two orders of magnitude. This means that heat flows down the fibers much faster than in the poorly conducting matrix. Because of this, temperature gradients at the fiber-matrix interface become significant and heat flows to the matrix from the fibers. As a consequence, heat transfer along the fibers and the matrix is no longer independent, but coupled: heat flow is longitudinal *and* transverse.

Nevertheless, Taylor et al. [24] and Balageas et al. [25] have determined three criteria for which the idea of effective longitudinal thermal diffusivity in fiber-reinforced composites is valid. As mentioned above these are:

1. sample axial dimension must be much larger than the radial fiber dimension;
2. thermal barrier between fiber and matrix must be negligible;
3. fiber volume fraction must high.

Assuming sample thickness (condition 1) and fiber volume fraction (condition 3) are fixed, the critical parameter to determine homogeneity is contact conductance. For purposes of discussion, the following will focus on the application of the Parker et al. [22]

flash method. Based on physical grounds, the contact thermal conductance will have a value somewhere between 0 (infinite thermal resistance) and ∞ (perfect thermal contact).

Perfect thermal contact

After the pulse of energy is absorbed by the composite on a side normal to the fibers, two types of heat fronts will be created. One type will diffuse down the fibers, and the other will travel along the matrix. However, since a high *longitudinal* thermal resistance exists in the matrix, the energy in the matrix will immediately move to the fibers where the thermal resistance is much lower. These thermal *longitudinal* resistances are not be confused with the *contact* thermal resistance at the fiber-matrix interface. This means that the matrix temperature will remain the initial temperature until the heat front in the fibers arrives. As most of the energy flows down the fibers, large thermal gradients will be created at the fiber-matrix interface. Since there is perfect thermal contact, $T_{fiber} = T_{matrix}$ (at the interface), and because the fiber volume fraction is high (>50%) heat diffused from the fibers into the matrix to meet the boundary condition will render the temperature of the matrix equal to that of the fibers. Because of this an apparent uniform heat front will develop in the composite. This is why homogeneity will develop if the three criteria presented above are met. According to Hasselman et al. [26], if these conditions are satisfied, the effective thermal conductivity for the composite, k_e is given by:

$$k_e = \alpha_{mes}(\rho_m c_m v_m + \rho_f c_f v_f) \tag{1-4}$$

where the subscripts *mes*, *m*, and *f* refer to the measured value, the matrix, and the fiber respectively. v is the volume fraction.

No thermal contact

The situation changes dramatically if the thermal resistance between the fibers and the matrix approaches infinity. Just as with the previous case, two heat fronts will be created after the energy pulse is deposited in the composite. However, under this new condition the heat flow in the matrix and in the fibers will be completely independent. Since the conductivity of the fiber is much higher than that of the matrix, the fiber heat front will diffuse to the opposite end of the sample much quicker than the matrix heat front. Within the context of the flash diffusivity method, the temperature rise at the back face will be caused exclusively by the fibers, without any contribution from the matrix. This is not to say that the temperature of the matrix at the back face will never rise. Eventually the matrix heat front will reach the opposite end of the sample, but it will take orders of magnitude more time to do so compared with the fiber heat front. This means the flash method could be used to measure the diffusivity of the fibers only. In this case the idea of an effective thermal diffusivity for the composite becomes ambiguous if not erroneous.

A perfect thermal barrier will never be achieved between the matrix and the fiber of a composite. This would require the complete absence of contact between the two phases. In other words the fibers would have to "levitate" in the matrix. Even then, heat transfer would occur due to conduction and radiation through the gaseous medium between the fibers and the matrix and some type of thermal contact would be established.

Perfect thermal contact between the fibers and the matrix is not expected to occur either. During manufacture the temperature of a newly made laminated composite can reach into the hundreds of degrees Celsius. During cooling the fibers and the matrix will contract at different rates according to their respective thermal expansion coefficients. This leads to small gaps between the fibers and the matrix at the interface, and therefore to a finite contact thermal conductance.

Summary

According to Taylor et al. [24] and Balageas et al. [25] three conditions must be met if laminated composite materials are to be considered homogeneous in the longitudinal direction for the purpose of transient thermal diffusivity measurements. For the scope of this work two of these criteria are satisfied -- as discussed above. Therefore, the critical parameter to determine homogeneity is the thermal contact conductance. If the conductance is large, the effective longitudinal thermal conductivity becomes a valid concept for laminated composites. As discussed, thermal contacts between fibers and matrix are never perfect. This raises a question regarding the minimum value for the contact conductance that will result in reliable temperature data from which to determine effective thermal diffusivity and thermal conductivity in fiber-reinforced composites. The main purpose of the rest of this work is to answer this question.

CHAPTER 2

2.1 Statement of the Problem

The question posed in Chapter 1 regarding the role of the thermal contact conductance is analyzed in this chapter by means of a theoretical approach. The mathematical model consists of a single cylindrical fiber surrounded by a hollow cylinder or shell, which represents the matrix. The boundary conditions are chosen to simulate a typical flash experiment. The details of the flash method were discussed in Chapter 1, but are repeated here for convenience. The energy is deposited in the composite at $x = L$ by means of a lamp or laser pulse of very short duration (about 1ms). The heat

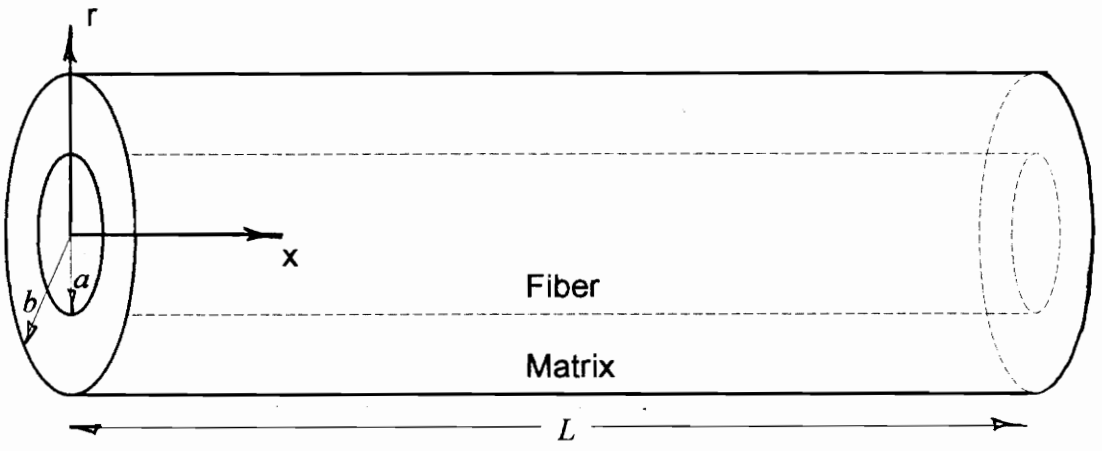

Figure 2-1 Mathematical model of the composite.

diffuses down the fibers and the matrix, and the temperature rise at the back face, $x = 0$, is measured in order to estimate the thermal diffusivity of the composite. Figure 2-1 shows the details of the model.

Note that only one fiber is considered in this analysis. The amount of matrix surrounding the fiber is determined by the fiber to matrix volume-ratio. In actual samples there are many thousand fibers surrounded by matrix, but since we are assuming that all the fibers have similar thermal behavior, the knowledge of the temperature field in one fiber-matrix unit describes the temperature in the entire composite sample.

The governing equations are

$$\alpha_f \frac{1}{r}\frac{\partial}{\partial r}\left(r\frac{\partial T_f}{\partial r}\right) + \alpha_f \frac{\partial^2 T_f}{\partial x^2} = \frac{\partial T_f}{\partial t} \qquad \text{in } 0 < r < a, \qquad (2\text{-}1a)$$

$$\alpha_m \frac{1}{r}\frac{\partial}{\partial r}\left(r\frac{\partial T_m}{\partial r}\right) + \alpha_m \frac{\partial^2 T_m}{\partial x^2} = \frac{\partial T_m}{\partial t} \qquad \text{in } a < r < b, \qquad (2\text{-}1b)$$

subject to the boundary conditions

$$\frac{\partial T_i}{\partial x} = 0 \qquad \text{at } x=0, \qquad (2\text{-}2a)$$

$$k_i \frac{\partial T_i}{\partial x} + hT_i = q''(t) \qquad \text{at } x=L, \qquad (2\text{-}2b)$$

$$-k_f \frac{\partial T_f}{\partial r} = h_c(T_f - T_m) = -k_m \frac{\partial T_m}{\partial r} \qquad \text{at } r=a, \qquad (2\text{-}2c)$$

and

$$\frac{\partial T_m}{\partial r} = 0 \qquad \text{at } r=b, \qquad (2\text{-}2d)$$

and the initial conditions

$$T_f = 0 \qquad \text{for } t=0, \qquad \text{(2-3a)}$$

$$T_m = 0 \qquad \text{for } t=0, \qquad \text{(2-3b)}$$

where m refers to the matrix, f refers to the fiber, and i represents either. Note that the material properties are assumed to be constant. In order to develop an appreciation for the mathematical difficulty of this problem, in the next two sections two popular analytical methods are used to try to solve (2-1)-(2-3). Both the integral-transform method and the separation of variables method fail to produce solutions, but it is worthwhile to go through the solution method to demonstrate why these methods do not to generate the required temperature fields.

2.2 Integral-Transform Technique

In this section we use the integral transform technique to try to solve equations (2-1) along with boundary conditions (2-2) and initial conditions (2-3). In this method the second partial derivatives with respect to the space variables are removed from the partial differential equation by the application of integral transforms. Therefore the problem is reduced to a first-order ordinary differential equation in time for the transform of the temperature. This ordinary differential equation is solved subject to the transformed initial condition, and the result is inverted successively to obtain the solution for the temperature. The development shown here is largely based on the work of Mulholland et al. [8] and Ozisik [27].

Development of eigenfunctions

Assume solutions of the form:

$$T_f(x,r,t) = X_f(x)R_f(r)\Gamma_f(t); \tag{2-4a}$$

$$T_m(x,r,t) = X_m(x)R_m(r)\Gamma_m(t). \tag{2-4b}$$

Substitute equations (2-4) into (2-1). Equation (2-1a) then becomes

$$\alpha_f \frac{1}{R_f}\frac{1}{r}\frac{d}{dr}(r\frac{dR_f}{dr}) + \alpha_f \frac{1}{X_f}\frac{d^2X_f}{dx^2} = \frac{1}{\Gamma_f}\frac{d\Gamma_f}{dt}, \tag{2-5a}$$

and equation (2-1b) becomes

$$\alpha_m \frac{1}{R_m}\frac{1}{r}\frac{d}{dr}(r\frac{dR_m}{dr}) + \alpha_m \frac{1}{X_m}\frac{d^2X_m}{dx^2} = \frac{1}{\Gamma_m}\frac{d\Gamma_m}{dt}. \tag{2-5b}$$

Thus the variables have been separated in equation (2-1). Since x, r, and t are independent the only way equation (2-5) can be satisfied is by letting each of the spatial terms be equal to a different constant. Anticipating that the differential equations in r will share the same eigenvalues because of boundary condition (2-2c), and that the differential equations in x will not, it follows that

$$\alpha_i \frac{1}{R_i}\frac{1}{r}\frac{d}{dr}\left(r\frac{dR_i}{dr}\right) = -\lambda^2; \tag{2-6}$$

$$\alpha_f \frac{1}{X_f}\frac{d^2X_f}{dx^2} = -\beta^2; \tag{2-7}$$

$$\alpha_m \frac{1}{X_m}\frac{d^2X_m}{dx^2} = -\eta^2. \tag{2-8}$$

Now consider the homogeneous version of boundary conditions (2-2) and assume that the variables separate. Three different eigenproblems develop. For each radial contribution R_i, we have

$$\frac{1}{r}\frac{d}{dr}\left(r\frac{dR_i}{dr}\right) + \frac{\lambda^2}{\alpha_i}R_i = 0, \tag{2-9}$$

$$\left|R_f(0)\right| < \infty, \tag{2-10a}$$

$$-k_f\frac{dR_f}{dr} = h_c(R_f - R_m) = -k_m\frac{dR_m}{dr} \qquad \text{at } r=a, \tag{2-10b}$$

and

$$\frac{dR_m}{dr} = 0 \qquad \text{at } r=b. \tag{2-10c}$$

For the axial fiber contribution, X_f , we have

$$\frac{d^2X_f}{dx^2}+\frac{\beta^2}{\alpha_f}X_f=0, \tag{2-11}$$

$$\frac{dX_f}{dx}=0 \qquad \text{at } x=0, \tag{2-12a}$$

and

$$k_f\frac{dX_f}{dx}+hX_f=0 \qquad \text{at } x=L. \tag{2-12b}$$

And finally for the matrix axial contribution, X_m,

$$\frac{d^2X_m}{dx^2}+\frac{\eta^2}{\alpha_m}X_m=0, \tag{2-13}$$

$$\frac{dX_m}{dx}=0 \qquad \text{at } x=0, \tag{2-14a}$$

and

$$k_m\frac{dX_m}{dx}+hX_m=0 \qquad \text{at } x=L. \tag{2-14b}$$

Equation (2-9) is Bessel's differential equation of order 0. The general solution for the two regions can be written [28]

$$R_{fn}=A_{1n}J_o(\frac{\lambda_n}{\sqrt{\alpha_f}}r)+A_{2n}Y_o(\frac{\lambda_n}{\sqrt{\alpha_f}}r) \qquad \text{in } 0<r<a, \tag{2-15a}$$

$$R_{mn}=B_{1n}J_o(\frac{\lambda_n}{\sqrt{\alpha_m}}r)+B_{2n}Y_o(\frac{\lambda_n}{\sqrt{\alpha_m}}r) \qquad \text{in } a<r<b. \tag{2-15b}$$

The index arises from the fact that equation (2-9) along with boundary condition (2-10) is a boundary-value problem and an infinite number of λ's satisfy the equation. The constants A_{1n}, A_{2n}, B_{1n}, and B_{2n} can be evaluated using (2-10). Similarly for equations (2-11) and (2-13), it is found that

$$X_{fp} = A_{1p}\sin(\frac{\beta_p}{\sqrt{\alpha_f}}x) + B_{2p}\cos(\frac{\beta_p}{\sqrt{\alpha_f}}x) \qquad \text{in } 0 < x < L, \tag{2-16}$$

$$X_{mj} = A_{1j}\sin(\frac{\eta_j}{\sqrt{\alpha_m}}x) + B_{2j}\cos(\frac{\eta_j}{\sqrt{\alpha_m}}x) \qquad \text{in } 0 < x < L. \tag{2-17}$$

It follows that for Γ_m and Γ_f,

$$\frac{1}{\Gamma_f}\frac{d\Gamma_f}{dt} = -\beta_p^2 - \lambda_n^2; \tag{2-18}$$

$$\frac{1}{\Gamma_m}\frac{d\Gamma_m}{dt} = -\eta_j^2 - \lambda_n^2. \tag{2-19}$$

The solutions are readily obtained as

$$\Gamma_{fpn} = e^{-(\beta_p^2+\lambda_n^2)t}; \tag{2-20}$$

$$\Gamma_{mjn} = e^{-(\eta_j^2+\lambda_n^2)t}. \tag{2-21}$$

Development of transform pairs

Consider the representation of the function $T_i(x,r,t)$ in the interval $0 < x < L$, defined for the matrix and the fiber, in the form

$$T_f(x,r,t) = \sum_{p=1}^{\infty} c_{fp}(r,t)X_{fp}(x); \tag{2-22}$$

$$T_m(x,r,t)=\sum_{j=1}^{\infty} c_{mj}(r,t)X_{mj}(x). \tag{2-23}$$

To determine the unknown coefficients c_{fp} and c_{mj}, we operate on both sides of these equations with $\int_0^L X_{ih}dx$ to find

$$\int_0^L X_f(\beta_h)T_f(x,r,t)dx=\sum_{p=1}^{\infty} c_{fp}(r,t)\int_0^L X_f(\beta_h)X_f(\beta_p)dx, \tag{2-24}$$

$$\int_0^L X_m(\eta_h)T_m(x,r,t)dx=\sum_{j=1}^{\infty} c_{mj}(r,t)\int_0^L X_m(\eta_h)X_m(\eta_j)dx. \tag{2-25}$$

The eigenfunctions X_m and X_f defined by the eigenproblems (2-11), (2-12) and (2-13), (2-14) satisfy the orthogonality relation [29]

$$\int_0^L X_{ij}(x)X_{ih}(x)dx = N_j \text{ if } j=h$$

$$\int_0^L X_{ij}(x)X_{ih}(x)dx = 0 \quad \text{if } j\neq h$$

therefore,

$$\overline{T}_{fp}(r,t)=c_{fp}(r,t)N_{fp}(\beta_p) \text{ or } c_{fp}(r,t)=\frac{\overline{T}_{fp}(r,t)}{N_{fp}(\beta_p)}; \tag{2-26}$$

and

$$\overline{T}_{mj}(r,t)=c_{mj}(r,t)N_{mj}(\eta_j) \text{ or } c_{mj}(r,t)=\frac{\overline{T}_{mj}(r,t)}{N_{mj}(\eta_j)}. \tag{2-27}$$

Here $N_j=\int_0^L X_{ij}^2dx$ is the normalization integral and $\overline{T}_i(r,t)=\int_0^L X_iT_i(x,r,t)dx$ is the integral transform of the function $T_i(x,r,t)$ with respect to the space variable x.

Now consider the representation of the function $\overline{T}_i(r,t)$ in the interval $0 < r < b$, defined for the matrix and the fiber in the form

$$\overline{T}_{fn}(r,t) = \sum_{n=1}^{\infty} b_{fn}(t)\, R_{fn}(r); \tag{2-28}$$

$$\overline{T}_{mn}(r,t) = \sum_{n=1}^{\infty} b_{mn}(t)\, R_{mn}(r). \tag{2-29}$$

To determine the unknown coefficients we operate on both sides of these equations with $\int_i \frac{k_i}{\alpha_i} r R_i dr$ and add the resulting expressions to obtain

$$\int_0^a \frac{k_f}{\alpha_f} r R_{fl} \overline{T}_{fl} dr + \int_a^b \frac{k_m}{\alpha_m} r R_{ml} \overline{T}_{ml} dr = \sum_{n=1}^{\infty} b_n(t) \left[\int_0^a \frac{k_f}{\alpha_f} r R_{fn} R_{fl} dr + \int_a^b \frac{k_m}{\alpha_m} r R_{mn} R_{ml} dr \right]. \tag{2-30}$$

The eigenfunctions R_i defined by the eigenproblem (2-9), (2-10) satisfy the orthogonality relation [30]

$$\begin{aligned} &\int_0^a \frac{k_f}{\alpha_f} r R_{fn} R_{fl} dr + \int_a^b \frac{k_m}{\alpha_m} r R_{mn} R_{ml} dr = N_n \quad \text{if } n = l \\ &\int_0^a \frac{k_f}{\alpha_f} r R_{fn} R_{fl} dr + \int_a^b \frac{k_m}{\alpha_m} r R_{mn} R_{ml} dr = 0 \quad \text{if } n \neq l \end{aligned} \tag{2-31}$$

where the normalization integral is defined as $N_n = \int_0^a \frac{k_f}{\alpha_f} r R_{fn}^2 dr + \int_a^b \frac{k_m}{\alpha_m} r R_{mn}^2 dr$. By virtue of this orthogonality relation, equation (2-30) becomes

$$\int_0^a \frac{k_f}{\alpha_f} \overline{T}_{fl} r R_{fl} dr + \int_a^b \frac{k_m}{\alpha_m} \overline{T}_{ml} r R_{ml} dr = \overline{\overline{T}}_l(t) = b_l(t) N_l. \tag{2-32}$$

Changing the index back to n and solving for $b_n(t)$, we find

$$b_n(t) = \frac{\overline{\overline{T}}_n(t)}{N_n}. \tag{2-33}$$

$\overline{\overline{T}}_n(t)$ in equation (2-33) is the integral transform of the functions $\overline{T}_{fn}$ and $\overline{T}_{mn}$ with respect to the variable *r*. The integral transform pairs can now be written. Equations (2-26) and (2-27) are introduced into equations (2-22) and (2-23) and equation (2-33) is introduced into (2-28) and (2-29) to yield the following relations:

Inversion formula: $$\overline{T}_{in}(r,t) = \sum_{n=1}^{\infty} \frac{\overline{\overline{T}}_n(t)}{N_n} R_{in}(r) \tag{2-34}$$

Integral transform: $$\overline{\overline{T}}_n(t) = \int_0^a \frac{k_f}{\alpha_f} \overline{T}_{fn} r R_{fn} dr + \int_a^b \frac{k_m}{\alpha_m} \overline{T}_{mn} r R_{mn} dr \tag{2-35}$$

Inversion formula: $$T_f(x,r,t) = \sum_{l=1}^{\infty} \frac{\overline{T}_{il}(r,t)}{N_l} X_{il}(x) \tag{2-36}$$

Integral transform: $$\overline{T}_{il}(r,t) = \int_0^L X_{il} T_i(x,r,t) dx \tag{2-37}$$

Integral transformation of the governing equation

Having established the appropriate integral transform pairs, the next step in the analysis is the removal of the partial derivatives with respect to the space variables in (2-1) by the application of transforms (2-35) and (2-37). The partial differentiation with respect to *x* will be removed first by multiplying both sides of equation (2-1) by the operator $\int_0^L X_i dx$ to yield

$$\int_0^L \alpha_i \frac{1}{r} \frac{\partial}{\partial r} (r \frac{\partial T_i}{\partial r}) X_i dx + \int_0^L \alpha_i \frac{\partial^2 T_i}{\partial x^2} X_i dx = \int_0^L \frac{\partial T_i}{\partial t} X_i dx. \tag{2-38}$$

By using the definition of the integral transform (2-37), we find

$$\alpha_i \frac{1}{r}\frac{\partial}{\partial r}(r\frac{\partial \overline{T}_i}{\partial r}) + \int_0^L \alpha_i \frac{\partial^2 T_i}{\partial x^2} X_i dx = \frac{\partial \overline{T}_i}{\partial t}. \tag{2-39}$$

The second term in equation (2-39) can be evaluated by using integration by parts and boundary conditions (2-2a) and (2-2b) as follows:

$$\int_0^L \alpha_i \frac{\partial^2 T_i}{\partial x^2} X_i dx = uv - \int v du. \tag{2-40}$$

Let $u = X_i$, $dv = \alpha_i \frac{\partial^2 T_i}{\partial x^2} dx$; then equation (2-40) becomes

$$\int_0^L \alpha_i \frac{\partial^2 T_i}{\partial x^2} X_i dx = X_i \alpha_i \frac{\partial T_i}{\partial x}\Big|_0^L - \int_0^L \alpha_i \frac{\partial T_i}{\partial x}\frac{dX_i}{dx} dx. \tag{2-41}$$

In order to evaluate the second term of (2-41) we use integration by parts again and let $u = \frac{dX_i}{dx}$, $dv = \alpha_i \frac{\partial T_i}{\partial x} dx$, yielding

$$\int_0^L \alpha_i \frac{\partial^2 T_i}{\partial x^2} X_i dx = X_i \alpha_i \frac{\partial T_i}{\partial x}\Big|_0^L - \alpha_i \frac{dX_i}{dx} T_{i0}^L + \int_0^L \alpha_i T_i \frac{d^2 X_i}{dx^2} dx. \tag{2-42}$$

By using boundary conditions (2-2a), (2-2b) and differential equation (2-10), we find

$$\int_0^L \alpha_i \frac{\partial^2 T_i}{\partial x^2} X_i dx = X_i(L)\alpha_i\left[\frac{q''(t)}{k_i} - \frac{h}{k_i} T_i(L)\right] - \alpha_i\left[-\frac{h}{k_i} X_i(L)\right] T_i(L) + \int_0^L \alpha_i T_i\left[-\frac{(\beta \text{ or } \eta)^2}{\alpha_i} X_i\right] dx. \tag{2-43}$$

This expression reduces to

$$\int_0^L \alpha_i \frac{\partial^2 T_i}{\partial x^2} X_i dx = \frac{\alpha_i}{k_i} X_i(L) q''(t) - (\beta \text{ or } \eta)^2 \overline{T}_i. \tag{2-44}$$

Introducing this result into (2-39), it follows that

$$\alpha_i \frac{1}{r}\frac{\partial}{\partial r}(r\frac{\partial \overline{T}_i}{\partial r}) + \frac{\alpha_i}{k_i} X_i(L) q''(t) - (\beta \text{ or } \eta)^2 \overline{T}_i = \frac{\partial \overline{T}_i}{\partial t}. \tag{2-45}$$

Now the partial derivative with respect to r will be removed by multiplying both sides of (2-45) by the operator $\int_i \frac{k_i}{\alpha_i} r R_i dr$ and adding the resulting expressions as follows:

$$\int_0^a k_f R_f \frac{\partial}{\partial r}(r\frac{\partial \overline{T}_f}{\partial r})dr + \int_a^b k_m R_m \frac{\partial}{\partial r}(r\frac{\partial \overline{T}_m}{\partial r})dr + X_i(L) q''(t)\left[\int_0^a r R_f dr + \int_a^b r R_m dr\right]$$
$$-\frac{k_f}{\alpha_f}\beta^2 \int_0^a \overline{T}_f r R_f dr - \frac{k_m}{\alpha_m}\eta^2 \int_0^a \overline{T}_m r R_m dr = \frac{d\overline{\overline{T}}}{dt}. \tag{2-46}$$

The first two terms can be evaluated by using Green's theorem, the radial boundary conditions and the definition of the integral transform (2-35) [31]; this yields

$$q''(t) X_i(L)\left[\int_0^a r R_f dr + \int_a^b r R_m dr\right] - \lambda^2 \overline{\overline{T}} - \left[\frac{k_f}{\alpha_f}\beta^2 \int_0^a \overline{T}_f r R_f dr + \frac{k_m}{\alpha_m}\eta^2 \int_a^b \overline{T}_m r R_m dr\right] = \frac{d\overline{\overline{T}}}{dt}. \tag{2-47}$$

Comparing the third term of this result with the integral transform (2-35), we see that they are almost identical except for the fact that the eigenvalues for the fiber and for the matrix are multiplying their respective integrals in (2-47). Because of this, the transformation cannot be executed and a closed-form solution cannot be obtained using this method. However, according to the development of Ozisik [27], an explicit solution is possible for this type of problem. Yet clearly, in order to complete the problem using (2-47), β and η must be equal. In other words, a single eigenvalue must satisfy the eigenproblems for the fiber and for the matrix. In the radial direction a single eigenvalue, λ, describes both regions, but this is because the eigensolutions are coupled through the

boundary condition at $r=a$. However, the eigenproblems for the axial direction are independent and are not coupled at any boundary. This requires the use of two independent eigenvalues for each region which in general are *different*. Therefore a solution cannot be achieved by the integral-transform method for problem (2-1) with boundary conditions (2-2) and initial conditions (2-3). When authors in the literature test their "general" results regarding problems of the type described above they use one-dimensional models for the sake of simplicity. It is clear that a one-dimensional model will yield closed-form solutions, but apparently not two-dimensional models for which one spatial dimension is not coupled. The present author has not seen any works that show how to proceed in this case in *detail*.

2.3 Application of Duhamel's Theorem

Since the integral-transform method does not work for the problem of interest, the method of separation of variables and Duhamel's theorem [32] will be attempted in this section. The statement of the problem is repeated here for convenience.

The governing equations are:

$$\frac{1}{r}\frac{\partial}{\partial r}(r\frac{\partial T_f}{\partial r})+\frac{\partial^2 T_f}{\partial x^2}=\frac{1}{\alpha_f}\frac{\partial T_f}{\partial t} \qquad \text{in } 0<r<a, \qquad (2\text{-}1a)$$

$$\frac{1}{r}\frac{\partial}{\partial r}(r\frac{\partial T_m}{\partial r})+\frac{\partial^2 T_m}{\partial x^2}=\frac{1}{\alpha_m}\frac{\partial T_m}{\partial t} \qquad \text{in } a<r<b, \qquad (2\text{-}1b)$$

subject to the boundary conditions

$$\frac{\partial T_i}{\partial x}=0 \qquad \text{at } x=0, \qquad (2\text{-}2a)$$

$$\frac{\partial T_i}{\partial x}+\frac{h}{k_i}T_i=\frac{q''(t)}{k_i} \qquad \text{at } x=L, \qquad (2\text{-}2b)$$

$$-k_f\frac{\partial T_f}{\partial r}=h_c(T_f-T_m)=-k_m\frac{\partial T_m}{\partial r} \qquad \text{at } r=a, \qquad (2\text{-}2c)$$

and

$$\frac{\partial T_m}{\partial r}=0 \qquad \text{at } r=b, \qquad (2\text{-}2d)$$

and the initial conditions

$$T_f=0 \qquad \text{for } t=0, \qquad (2\text{-}3a)$$

$$T_m = 0 \qquad \text{for } t=0, \qquad (2\text{-}3b)$$

where m refers to the matrix, f refers to the fiber, and i represents either.

This problem is homogeneous except for boundary condition (2-2b). When a heat conduction problem is non-homogeneous due to a boundary condition, it can be split up into two problems that may be solved by separation of variables. However, the non-homogeneous boundary conditions must not depend on time. The fact that boundary condition (2-2b) depends on time does not represent any difficulty. Duhamel's theorem [32] can be used to relate the solution of problem (2-1) with time-independent boundary conditions to the actual problem of time-dependent boundary conditions. First an auxiliary problem needs to be defined:

$$\frac{1}{r}\frac{\partial}{\partial r}\left(r\frac{\partial \Phi_f}{\partial r}\right)+\frac{\partial^2 \Phi_f}{\partial x^2}=\frac{1}{\alpha_f}\frac{\partial \Phi_f}{\partial t} \qquad \text{in } 0<r<a, \qquad (2\text{-}48a)$$

$$\frac{1}{r}\frac{\partial}{\partial r}\left(r\frac{\partial \Phi_m}{\partial r}\right)+\frac{\partial^2 \Phi_m}{\partial x^2}=\frac{1}{\alpha_m}\frac{\partial \Phi_m}{\partial t} \qquad \text{in } a<r<b, \qquad (2\text{-}48b)$$

subject to the boundary conditions

$$\frac{\partial \Phi_i}{\partial x}=0 \qquad \text{at } x=0, \qquad (2\text{-}49a)$$

$$\frac{\partial \Phi_i}{\partial x}+\frac{h}{k_i}\Phi_i=\frac{1}{k_i} \qquad \text{at } x=L, \qquad (2\text{-}49b)$$

$$-k_f\frac{\partial \Phi_f}{\partial r}=h_c(\Phi_f-\Phi_m)=-k_m\frac{\partial \Phi_m}{\partial r} \qquad \text{at } r=a, \qquad (2\text{-}49c)$$

and

$$\frac{\partial \Phi_m}{\partial r} = 0 \qquad \text{at } r=b, \qquad (2\text{-}49d)$$

and the initial conditions

$$\Phi_f = 0 \qquad \text{for } t=0, \qquad (2\text{-}50a)$$

$$\Phi_m = 0 \qquad \text{for } t=0. \qquad (2\text{-}50b)$$

Then, the solution $T_i(x,r,t)$ of problem (2-1), (2-2), and (2-3) is related to the solution of $\Phi_i(x,r,t)$ by [33]

$$T_i(x,r,t) = \int_{\tau=0}^{t} q''(\tau) \frac{\partial \Phi_i(x,r,t-\tau)}{\partial t} d\tau \qquad (2\text{-}51)$$

Now since problem (2-48)-(2-50) does not have boundary conditions that depend on time, a solution based on separation of variables can proceed. Problem (2-48)-(2-50) will be split into a homogeneous unsteady problem and a steady-state problem which contains the non-homogeneous boundary condition.

Steady-state problem

$$\frac{1}{r}\frac{\partial}{\partial r}\left(r\frac{\partial \Phi_{i,o}}{\partial r}\right) + \frac{\partial^2 \Phi_{i,o}}{\partial x^2} = 0, \qquad (2\text{-}52)$$

subject to the boundary conditions

$$\frac{\partial \Phi_{i,o}}{\partial x} = 0 \qquad \text{at } x=0, \qquad (2\text{-}53a)$$

$$\frac{\partial \Phi_{i,o}}{\partial x} + \frac{h}{k_i}\Phi_{i,o} = \frac{1}{k_i} \qquad \text{at } x=L, \qquad (2\text{-}53b)$$

$$-k_f \frac{\partial \Phi_{f,o}}{\partial r} = h_c(\Phi_{f,o} - \Phi_{m,o}) = -k_m \frac{\partial \Phi_{m,o}}{\partial r} \quad \text{at } r=a, \tag{2-53c}$$

and

$$\frac{\partial \Phi_{m,o}}{\partial r} = 0 \quad \text{at } r=b. \tag{2-53d}$$

Unsteady problem

$$\frac{1}{r}\frac{\partial}{\partial r}(r\frac{\partial \Phi_{i,h}}{\partial r}) + \frac{\partial^2 \Phi_{i,h}}{\partial x^2} = \frac{1}{\alpha_i}\frac{\partial \Phi_{i,h}}{\partial t}, \tag{2-54}$$

subject to the boundary conditions

$$\frac{\partial \Phi_{i,h}}{\partial x} = 0 \quad \text{at } x=0, \tag{2-55a}$$

$$\frac{\partial \Phi_{i,h}}{\partial x} + \frac{h}{k_i}\Phi_{i,h} = 0 \quad \text{at } x=L, \tag{2-55b}$$

$$-k_f \frac{\partial \Phi_{f,h}}{\partial r} = h_c(\Phi_{f,h} - \Phi_{m,h}) = -k_m \frac{\partial \Phi_{m,h}}{\partial r} \quad \text{at } r=a, \tag{2-55c}$$

and

$$\frac{\partial \Phi_{m,h}}{\partial r} = 0 \quad \text{at } r=b, \tag{2-55d}$$

and the initial conditions

$$\Phi_{i,h} = -\Phi_{i,o} \quad \text{at } t=0. \tag{2-56}$$

The total solution is given by $\Phi_i(x,r,t) = \Phi_{i,h}(x,r,t) + \Phi_{i,o}(x,r)$.

Solution of the steady-state problem

Let $\Phi_{i,o}(x,r) = X_{i,o}(x)R_{i,o}(r)$ and substitute into equation (2-52):

$$\frac{1}{R_{i,o}}\frac{1}{r}\frac{d}{dr}\left(r\frac{dR_{i,o}}{dr}\right) + \frac{1}{X_{i,o}}\frac{d^2X_{i,o}}{dx^2} = 0. \tag{2-57}$$

Since $X_{i,o}(x)$ and $R_{i,o}(r)$ are independent, it is apparent that each term of (2-57) is constant. Furthermore, we choose the separation constant to produce an eigenproblem in the radial direction. This procedure yields one ordinary differential equation in x, viz.

$$\frac{1}{X_{i,o}}\frac{d^2X_{i,o}}{dx^2} = \gamma^2 \quad \text{or} \quad \frac{d^2X_{i,o}}{dx^2} - \gamma^2 X_{i,o} = 0, \tag{2-58}$$

subject to the boundary condition

$$\frac{dX_{i,o}}{dx} = 0 \qquad \text{at } x=0, \tag{2-59}$$

and an eigenproblem in r:

$$\frac{1}{R_{i,o}}\frac{1}{r}\frac{d}{dr}\left(r\frac{dR_{i,o}}{dr}\right) = -\gamma^2 \quad \text{or} \quad \frac{1}{r}\frac{d}{dr}\left(r\frac{dR_{i,o}}{dr}\right) + \gamma^2 R_{i,o} = 0, \tag{2-60}$$

subject to boundary conditions

$$\left|R_f(0)\right| < \infty, \tag{2-61a}$$

$$-k_f\frac{dR_{f,o}}{dr} = h_c(R_{f,o} - R_{m,o}) = -k_m\frac{dR_{m,o}}{dr} \qquad \text{at } r=a, \tag{2-61b}$$

and

$$\frac{dR_{m,o}}{dr} = 0 \qquad \text{at } r=b. \qquad (2\text{-}61c)$$

The solution to (2-58), (2-59) is $X_{i,o} = \cosh(\gamma_j x)$. The index comes from the fact that equation (2-60) along with boundary conditions (2-61) is a boundary-value problem and has an infinite number of solutions. The general solution for (2-60) is

$$R_{f,o} = A_{1j} J_0(\gamma_j r) + B_{1j} Y_0(\gamma_j r) \qquad \text{in } 0 < r < a, \qquad (2\text{-}62)$$

$$R_{m,o} = A_{2j} J_0(\gamma_j r) + B_{2j} Y_0(\gamma_j r) \qquad \text{in } a < r < b. \qquad (2\text{-}63)$$

Therefore the general solution can be written

$$\Phi_{i,o}(x,r) = \sum_{j=1}^{\infty} c_j \cosh(\gamma_j x) R_{i,o}(r). \qquad (2\text{-}64)$$

The constant in equation (2-64) can be evaluated using boundary condition (2-53b). Assuming term by term differentiation is valid, we find

$$\frac{\partial}{\partial x}\Phi_{i,o}(x,r) = \sum_{j=1}^{\infty} c_j \gamma_j \sinh(\gamma_j x) R_{i,o}(r), \qquad (2\text{-}65)$$

or, applying boundary condition (2-53b),

$$\frac{1}{k_i} = \sum_{j=1}^{\infty} c_j \gamma_j \sinh(\gamma_j L) R_{i,o}(r,\gamma_j) + \frac{h}{k_i} \sum_{j=1}^{\infty} c_j \cosh(\gamma_j L) R_{i,o}(r,\gamma_j). \qquad (2\text{-}66)$$

We operate on both sides of equation (2-66) with $k_i \int_i r R_{i,o} dr$ and add the resulting expressions to get

$$\int_0^a rR_{f,o}(\gamma_k)dr + \int_a^b rR_{m,o}(\gamma_k)dr =$$

$$\sum_{j=1}^{\infty} c_j \left[\gamma_j \sinh(\gamma_j L) + \frac{h}{k_i}\cosh(\gamma_j L) \right] \left[\int_0^a k_f rR_{f,o}(\gamma_j)R_{f,o}(\gamma_k)dr + \int_a^b k_m rR_{m,o}(\gamma_j)R_{m,o}(\gamma_k)dr \right].$$

(2-67)

Using the orthogonality property of the R eigenfunctions [similar to that of equation (2-31)], equation (2-67) becomes

$$\int_0^a rR_{f,o}(\gamma_k)dr + \int_a^b rR_{m,o}(\gamma_k)dr = c_k N_k \left[\gamma_k \sinh(\gamma_k L) + \frac{h}{k_i}\cosh(\gamma_k L) \right], \qquad (2\text{-}68)$$

where the normalization integral is defined as $N_k = \int_0^a k_f rR_{f,o}^2(\gamma_k)dr + \int_a^b k_m rR_{m,o}^2(\gamma_k)dr$.

Changing the index back to j and solving for the constant yields

$$c_j = \frac{\int_0^a rR_{f,o}(r,\gamma_j)dr + \int_a^b rR_{m,o}(r,\gamma_j)dr}{N_k \left[\gamma_k \sinh(\gamma_k L) + \frac{h}{k_i}\cosh(\gamma_k L) \right]}. \qquad (2\text{-}69)$$

The solution for the steady-state part then becomes

$$\Phi_{i,o}(x,r) = \sum_{j=1}^{\infty} \frac{\int_0^a rR_{f,o}(r,\gamma_j)dr + \int_a^b rR_{m,o}(r,\gamma_j)dr}{N_k \left[\gamma_k \sinh(\gamma_k L) + \frac{h}{k_i}\cosh(\gamma_k L) \right]} \cosh(\gamma_j x) R_{i,o}(r,\gamma_j). \qquad (2\text{-}70)$$

In order to have a complete solution, the constants in equations (2-62) and (2-63) and the corresponding eigenvalues must be evaluated using boundary conditions (2-61). It quickly follows that $B_{1,j}$ must vanish due to boundary condition (2-61a). Since boundary condition (2-61) represents a system of three linear, homogeneous equations the unknown

coefficients can only be determined in terms of any one of them. This means that one of the coefficients is arbitrary. We set $A_{1j} = 1$ for simplicity. This arbitrariness does not cause any difficulty because the arbitrary constant will appear in both the numerator and denominator of equation (2-70) and hence it will divide out. First the derivatives of (2-62) and (2-63) are found as follows:

$$\frac{dR_{f,o}}{dr} = -\gamma_j J_1(\gamma_j r) \tag{2-71}$$

$$\frac{dR_{m,o}}{dr} = -A_{2j}\gamma_j J_1(\gamma_j r) - B_{2j}\gamma_j Y_1(\gamma_j r). \tag{2-72}$$

By using boundary condition $\frac{dR_{m,o}}{dr} = 0$ at $r = b$ we have

$$A_{2j} = -\frac{Y_1(\gamma_j b)}{J_1(\gamma_j b)} B_{2j} \tag{2-73}$$

The remaining boundary condition, (2-61b), yields the other constant.

$$\frac{k_f}{k_m}\gamma_j J_1(\gamma_j a) = -\frac{Y_1(\gamma_j b)}{J_1(\gamma_j b)} B_{2j}\gamma_j J_1(\gamma_j a) + B_{2j}\gamma_j Y_1(\gamma_j a) \tag{2-74}$$

or

$$B_{2j} = \frac{k_f}{k_m} \frac{J_1(\gamma_j a)}{Y_1(\gamma_j a) - \frac{Y_1(\gamma_j b)}{J_1(\gamma_j b)} J_1(\gamma_j a)}. \tag{2-75}$$

Now apply boundary condition (2-61b) again to get.

$$k_f \gamma_j J_1(\gamma_j a) = h_c\left[J_0(\gamma_j a) - A_{2j} J_0(\gamma_j a) - B_{2j} Y_0(\gamma_j a)\right], \tag{2-76}$$

or

$$\frac{k_f}{h_c}\gamma_j J_1(\gamma_j a) = J_0(\gamma_j a) + \left\{\frac{Y_1(\gamma_j b)}{J_1(\gamma_j b)} J_0(\gamma_j a) - Y_0(\gamma_j a)\right\} \frac{k_f}{k_m} \frac{J_1(\gamma_j a)}{Y_1(\gamma_j a) - \frac{Y_1(\gamma_j b)}{J_1(\gamma_j b)} J_1(\gamma_j a)}. \tag{2-77}$$

Equation (2-77) yields the eigenvalues, γ_j, needed for the solution, and now the solution for the steady-state part of the problem is complete.

Solution to the unsteady problem

Let $\Phi_{i,h}(x,r,t) = X_{i,h}(x)R_{i,h}(r)\Gamma_{i,h}(t)$ and substitute into equation (2-54)

$$\frac{1}{R_{i,h}}\frac{1}{r}\frac{d}{dr}\left(r\frac{dR_{i,h}}{dr}\right) + \frac{1}{X_{i,h}}\frac{d^2X_{i,h}}{dx^2} = \frac{1}{\Gamma_{i,h}}\frac{d\Gamma_{i,h}}{dt}. \tag{2-78}$$

As before, each of the spatial terms in equation (2-78) must be constant, thus we write

$$\frac{1}{X_{i,h}}\frac{d^2X_{i,h}}{dx^2} = -\beta^2; \tag{2-79}$$

and

$$\frac{1}{R_{i,h}}\frac{1}{r}\frac{d}{dr}\left(r\frac{dR_{i,h}}{dr}\right) = -\lambda^2. \tag{2-80}$$

Equation (2-79) produces the following eigenproblem for x

$$\frac{d^2X_{i,h}}{dx^2} + \beta^2 X_{i,h} = 0, \tag{2-81}$$

subject to the boundary conditions

$$\frac{dX_{i,h}}{dx} = 0 \qquad \text{at } x = 0, \qquad (2\text{-}82a)$$

and

$$\frac{dX_{i,h}}{dx} + \frac{h}{k_i} X_{i,h} = 0 \qquad \text{at } x = L. \qquad (2\text{-}82b)$$

Equation (2-80) yields an eigenproblem for *r:*

$$\frac{1}{r}\frac{d}{dr}(r\frac{dR_{i,h}}{dr}) + \lambda^2 R_{i,h} = 0, \qquad (2\text{-}83)$$

subject to the boundary conditions

$$\left|R_{f,h}(0)\right| < \infty, \qquad (2\text{-}84a)$$

$$-k_f X_{f,h}\Gamma_{f,h}\frac{dR_{f,h}}{dr} = h_c(\Gamma_{f,h}X_{f,h}R_{f,o} - \Gamma_{m,h}X_{f,h}R_{m,o}) = -k_m X_{f,h}\Gamma_{m,h}\frac{dR_{m,o}}{dr} \text{ at } r=a, \qquad (2\text{-}84b)$$

and

$$\frac{dR_{m,h}}{dr} = 0 \qquad \text{at } r=b. \qquad (2\text{-}84c)$$

Since $\Gamma_{f,h}(t) = e^{-\alpha_f(\beta_p^2+\lambda_n^2)t} \neq \Gamma_{f,h}(t) = e^{-\alpha_m(\beta_p^2+\lambda_n^2)t}$ and $X_{f,h}(x) \neq X_{m,h}(x)$, boundary condition (2-84b) depends on *x*, *r* and *t*. Even though a general solution for (2-83) can be written as

$$R_{in} = A_{in}J_0(\lambda_n r) + B_{in}Y_0(\lambda_n r), \qquad (2\text{-}85)$$

when the "constants" are evaluated to meet the boundary conditions it becomes apparent that at least one of them will have to be a function of t and x in order to satisfy the time and spatial dependence of equation (2-84b). This means that at least one of the eigenfunctions $R_{f,h}$ and $R_{m,h}$ will depend on x and t. It follows that assumption (2-78) fails since the variables are *not* separable and a solution to problem (2-1), (2-2) and (2-3) is not possible through this method. Notice that this difficulty would also occur in the integral-transform method.

CHAPTER 3

3.1 Approximate Analytical Solution

Even though an analytical solution for the problem of interest is not achievable through the integral-transform method or the separation of variables method, a few simplifications can be made in order to obtain an approximate solution. As discussed in Chapter 1, one of the criteria required for homogeneity in laminated composites is that the length of the fibers in the axial direction be much larger than their dimension in the radial direction. A direct consequence of this is that the radial temperature gradients are negligible compared to gradients in the axial direction. This eliminates the r dependence in problem (2-1), (2-2), (2-3). However, in order to include the role of the contact conductance, h_c, energy transfer between the fibers and the matrix has to be considered in the new statement of the problem. Consider the cylindrical differential element (which represents the fiber) shown in Figure 3-1.

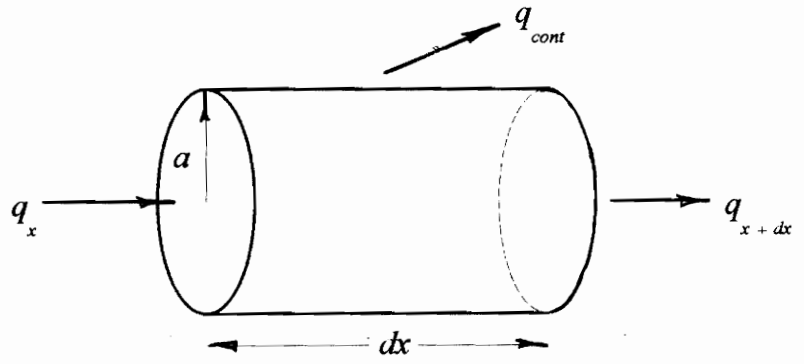

Figure 3-1 Fiber differential element.

Applying conservation of energy to the differential element,

$$q_x - q_{x+dx} - q_{cont} = \dot{q}_{st}, \tag{3-1}$$

where q_{cont} represents the heat transfer between the fiber and the matrix and $\dot{q}_{st}$ represents the change in stored energy. Expanding q_{x+dx} using Taylor's series and ignoring higher order terms, we have

$$q_{x+dx} = q_x + \frac{\partial q_x}{\partial x} dx. \tag{3-2}$$

Equation (3-1) then becomes,

$$-\frac{\partial q_x}{\partial x} dx - q_{cont} = \dot{q}_{st}. \tag{3-3}$$

Using Fourier's law, and expanding the individual terms in equation (3-3), we find

$$-\frac{\partial}{\partial x}\left(-k_f A_f \frac{\partial T_f}{\partial x}\right) dx - h_c 2\pi a dx (T_f - T_m) = \rho_f c_f A_f dx \frac{\partial T_f}{\partial t}, \tag{3-4}$$

or by dividing by dx,

$$-\frac{\partial}{\partial x}\left(-k_f A_f \frac{\partial T_f}{\partial x}\right) - h_c 2\pi a (T_f - T_m) = \rho_f c_f A_f \frac{\partial T_f}{\partial t}. \tag{3-5}$$

Since the cross sectional area A_f and the thermal conductivity are constant, the governing equation for the fiber becomes:

$$\frac{\partial}{\partial x}\left(\frac{\partial T_f}{\partial x}\right)-\frac{2h_c}{k_f a}(T_f-T_m)=\frac{1}{\alpha_f}\frac{\partial T_f}{\partial t}. \tag{3-6}$$

The corresponding boundary and initial conditions are

$$\frac{\partial T_f}{\partial x}=0 \qquad \text{at } x=0, \tag{3-7a}$$

$$k_f\frac{\partial T_f}{\partial x}+hT_f=q''(t) \qquad \text{at } x=L, \tag{3-7b}$$

$$T_f=0 \qquad \text{at } t=0 \tag{3-8}$$

Now consider a differential shell representing the matrix as shown in Figure 3-2.

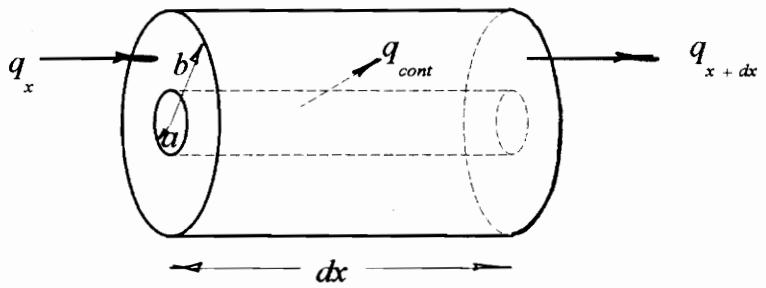

Figure 3-2 Matrix differential element.

Just as before, conservation of energy yields,

$$q_x-q_{x+dx}+q_{cont}=\dot{q}_{st}. \tag{3-9}$$

Using Taylor's series expansion and Fourier's law, we find

$$-\frac{\partial}{\partial x}\left(-k_m A_m\frac{\partial T_m}{\partial x}\right)dx+h_c 2\pi a dx(T_f-T_m)=\rho_m c_m A_m dx\frac{\partial T_m}{\partial t}. \tag{3-10}$$

Since the cross sectional area and properties are constant, the governing equation for the matrix becomes

$$\frac{\partial}{\partial x}\left(\frac{\partial T_m}{\partial x}\right)-\frac{2ah_c}{k_m(b^2-a^2)}(T_m-T_f)=\frac{1}{\alpha_m}\frac{\partial T_m}{\partial t}. \tag{3-11}$$

The appropriate boundary and initial conditions are

$$\frac{\partial T_m}{\partial x}=0 \qquad \text{at } x=0, \tag{3-12a}$$

$$k_m\frac{\partial T_m}{\partial x}+hT_m=q''(t) \qquad \text{at } x=L, \tag{3-12b}$$

$$T_m=0 \qquad \text{at } t=0. \tag{3-13}$$

Equations (3-6) and (3-11) have the form

$$\frac{\partial}{\partial x}\left(\frac{\partial T_i}{\partial x}\right)-l_i^2(T_i-T_{ii})=\frac{1}{\alpha_i}\frac{\partial T_i}{\partial t}, \tag{3-14}$$

where $l_f^2=\frac{2h_c}{k_f a}$ and $l_m^2=\frac{2ah_c}{k_m(b^2-a^2)}$, and ii represents the phase with which i is in contact through the conductance term. Equation (3-14), along with its boundary and initial conditions, can be solved using the integral-transform method. Consider the homogeneous version of equation (3-14) along with homogeneous boundary conditions,

$$\frac{\partial}{\partial x}\left(\frac{\partial T_i}{\partial x}\right)-l_i^2T_i=\frac{1}{\alpha_i}\frac{\partial T_i}{\partial t}; \tag{3-15}$$

$$\frac{\partial T_i}{\partial x} = 0 \qquad \text{at } x = 0, \qquad (3\text{-}16a)$$

$$k_i \frac{\partial T_i}{\partial x} + hT_i = 0 \qquad \text{at } x = L. \qquad (3\text{-}16b)$$

Assume a solution of the form

$$T_i(x,t) = X_i(x)\Gamma_i(t), \qquad (3\text{-}15)$$

and substitute into equation (3-15) to find

$$\Gamma_i \frac{d}{dx}\left(\frac{dX_i}{dx}\right) - l_i^2 \Gamma_i X_i = X_i \frac{1}{\alpha_i}\frac{d\Gamma_i}{dt}, \qquad (3\text{-}16)$$

or

$$\frac{1}{X_i}\frac{d}{dx}\left(\frac{dX_i}{dx}\right) - l_i^2 = \frac{1}{\Gamma_i}\frac{1}{\alpha_i}\frac{d\Gamma_i}{dt}. \qquad (3\text{-}17)$$

Setting the first term of this equation to $-\lambda_i^2$ yields the following eigenproblem:

$$\frac{d}{dx}\left(\frac{dX_i}{dx}\right) + \lambda_i^2 X_i = 0, \qquad (3\text{-}18)$$

subject to boundary conditions

$$\frac{dX_i}{dx} = 0 \qquad \text{at } x = 0, \qquad (3\text{-}19a)$$

$$k_i \frac{dX_i}{dx} + hX_i = 0 \qquad \text{at } x = L. \qquad (3\text{-}19b)$$

The solution to this boundary-value problem is given by

$$X_{im} = \cos(\lambda_{im} x), \tag{3-20}$$

where λ_{im} is the solution of

$$\lambda_{im} \tan(\lambda_{im} L) = \frac{h}{k_i} . \tag{3-21}$$

Now consider the representation of the function $T_i(x,t)$ in the interval $0 < x < L$ in terms of the eigenfunctions X_i:

$$T_i(x,t) = \sum_{m=1}^{\infty} c_m(t) X_{im}(x). \tag{3-22}$$

To determine the unknown coefficients, we operate on both sides of this equation with $\int_0^L X_i dx$ to find

$$\int_0^L T_i X_i(\lambda_{ij}) dx = \sum_{m=1}^{\infty} c_m(t) \int_0^L X_i(\lambda_{ij}) X_i(\lambda_{im}) dx . \tag{3-23}$$

The eigenfunctions X_i obey the following orthogonality relation [30]

$$\begin{aligned} &\int_0^L X_i(\lambda_{ij}) X_i(\lambda_{im}) dx = N_m \text{ if } m = j; \\ &\int_0^L X_i(\lambda_{ij}) X_i(\lambda_{im}) dx = 0 \quad \text{if } m \neq j. \end{aligned} \tag{3-24}$$

Therefore, equation (3-23) becomes

$$\int_0^L T_i X_i(\lambda_{ij})dx = \overline{T}_{ij}(t) = c_j(t)N_j, \tag{3-25}$$

where $\overline{T}_{ij}(t)$ is the integral transform of the function $T_i(x,t)$ with respect to the space variable x. By changing the index back to m and solving for $c_m(t)$, we have

$$c_m(t) = \frac{\overline{T}_{im}(t)}{N_m}. \tag{3-26}$$

Now the integral transform pair can be written as

$$\text{Inversion formula:} \quad T_i(x,t) = \sum_{m=1}^{\infty} \frac{\overline{T}_{im}(t)}{N_m} X_i(x,\lambda_{im}) \tag{3-27}$$

$$\text{Integral transform:} \quad \overline{T}_{im}(t) = \int_0^L T_i X_i(x,\lambda_{im})dx. \tag{3-28}$$

The next step in the analysis is the removal of the partial derivatives with respect to x in (3-14) by the application of the integral transform (3-28). Operate on both sides of the governing equation with $\int_0^L X_i dx$ to find

$$\int_0^L \frac{\partial}{\partial x}\left(\frac{\partial T_i}{\partial x}\right)X_i dx - l_i^2\left(\int_0^L T_i X_i dx - \int_0^L T_{ii} X_i dx\right) = \frac{1}{\alpha_i}\int_0^L \frac{\partial T_i}{\partial t} X_i dx. \tag{3-29}$$

Using the definition of the transform (3-28), equation (3-29) becomes

$$\int_0^L \frac{\partial}{\partial x}\left(\frac{\partial T_i}{\partial x}\right)X_i dx - l_i^2\left(\overline{T}_i - \int_0^L T_{ii} X_i dx\right) = \frac{1}{\alpha_i}\frac{d\overline{T}_i}{dt}. \tag{3-30}$$

The first term in this equation can be evaluated using integration by parts and by letting $u = X_i$ and $dv = \frac{\partial^2 T_i}{\partial x^2}$, viz

$$\int u dv = uv - \int v du \text{ or } \int_0^L \frac{\partial}{\partial x}\left(\frac{\partial T_i}{\partial x}\right) X_i dx = X_i \frac{\partial T_i}{\partial x}\Big|_0^L - \int_0^L \frac{\partial T_i}{\partial x}\frac{dX_i}{dx} dx. \quad (3\text{-}31)$$

We use integration by parts again, and let $u = \frac{dX_i}{dx}$, and $dv = \frac{\partial T_i}{\partial x} dx$ to find

$$\int_0^L \frac{\partial}{\partial x}\left(\frac{\partial T_i}{\partial x}\right) X_i dx = X_i \frac{\partial T_i}{\partial x}\Big|_0^L - \frac{dX_i}{dx} T_{i0}^L + \int_0^L T_i \frac{d^2 X_i}{dx^2} dx. \quad (3\text{-}32)$$

By using boundary conditions (3-19) and equation (3-18) it follows that

$$\int_0^L \frac{\partial}{\partial x}\left(\frac{\partial T_i}{\partial x}\right) X_i dx = X_i(L)\left[\frac{q''(t)}{k_i} - \frac{h}{k_i} T_i(L)\right] - \left[-\frac{h}{k_i} X_i(L)\right] T_i(L) + \int_0^L T_i(-\lambda_i^2 X_i) dx, \quad (3\text{-}34)$$

or by simplifying, we have

$$\int_0^L \frac{\partial}{\partial x}\left(\frac{\partial T_i}{\partial x}\right) X_i dx = X_i(L)\frac{q''(t)}{k_i} - \lambda_i^2 \overline{T}_i. \quad (3\text{-}34)$$

Substituting back into (3-30) yields

$$X_i(L)\frac{q''(t)}{k_i} - \lambda_i^2 \overline{T}_i - l_i^2(\overline{T}_i - \int_0^L T_{ii} X_i dx) = \frac{1}{\alpha_i}\frac{d\overline{T}_i}{dt}. \quad (3\text{-}35)$$

This is an ordinary differential equation for $\overline{T}_i(t)$, and it is easily solved. Rearranging, we have

$$\frac{d\overline{T}_i}{dt} + \alpha_i(\lambda_i^2 + l_i^2)\overline{T}_i = X_i(L)\frac{\alpha_i}{k_i} q''(t) + l_i^2 \alpha_i \int_0^L T_{ii} X_i dx. \quad (3\text{-}36)$$

Multiply both sides by the integrating factor $e^{\alpha_i(\lambda_i^2 + l_i^2)t}$ and simplify to find

$$\frac{d}{dt}\left[\overline{T}_i e^{\alpha_i(\lambda_i^2+l_i^2)t}\right] = e^{\alpha_i(\lambda_i^2+l_i^2)t} X_i(L)\frac{\alpha_i}{k_i} q"(t) + e^{\alpha_i(\lambda_i^2+l_i^2)t} l_i^2 \alpha_i \int_0^L T_{ii} X_i dx, \tag{3-37}$$

or,

$$d\left[\overline{T}_i e^{\alpha_i(\lambda_i^2+l_i^2)t}\right] = \left[e^{\alpha_i(\lambda_i^2+l_i^2)t} X_i(L)\frac{\alpha_i}{k_i} q"(t) + e^{\alpha_i(\lambda_i^2+l_i^2)t} l_i^2 \alpha_i \int_0^L T_{ii}(x,t) X_i dx \right] dt. \tag{3-38}$$

Integrating and using the transformed initial condition, we find

$$\overline{T}_i e^{\alpha_i(\lambda_i^2+l_i^2)t} = \int_0^t \left[e^{\alpha_i(\lambda_i^2+l_i^2)\xi} X_i(L)\frac{\alpha_i}{k_i} q"(\xi) + e^{\alpha_i(\lambda_i^2+l_i^2)\xi} l_i^2 \alpha_i \int_0^L T_{ii}(x,\xi) X_i dx \right] d\xi. \tag{3-39}$$

In order to integrate the first term, we assume that the energy is deposited in the composite in a uniform manner during a pulse of duration τ. Mathematically this can be expresed as

$$\begin{aligned} q"(\xi) &= q_o" \quad \text{for } \xi \le \tau; \\ q"(\xi) &= 0 \quad\quad \text{for } \xi > \tau. \end{aligned} \tag{3-40}$$

It follows that

$$\overline{T}_i e^{\alpha_i(\lambda_i^2+l_i^2)t} = X_i(L)\frac{\alpha_i}{k_i} q_o" \int_0^\tau e^{\alpha_i(\lambda_i^2+l_i^2)\xi} d\xi + l_i^2 \alpha_i \int_0^t \int_0^L X_i(x) e^{\alpha_i(\lambda_i^2+l_i^2)\xi} T_{ii}(x,\xi) dx d\xi, \tag{3-41}$$

or,

$$\overline{T}_i e^{\alpha_i(\lambda_i^2+l_i^2)t} = \frac{X_i(L) q_o"}{k_i(\lambda_i^2+l_i^2)}\left[e^{\alpha_i(\lambda_i^2+l_i^2)\tau} - 1 \right] + l_i^2 \alpha_i \int_0^t \int_0^L X_i(x) e^{\alpha_i(\lambda_i^2+l_i^2)\xi} T_{ii}(x,\xi) dx d\xi, \tag{3-42}$$

or,

$$\overline{T}_i(t) = \frac{X_i(L)q_o''}{k_i(\lambda_i^2 + l_i^2)}\left[e^{-\alpha_i(\lambda_i^2+l_i^2)(t-\tau)} - e^{-\alpha_i(\lambda_i^2+l_i^2)t}\right] + l_i^2\alpha_i\int_0^t\int_0^L X_i(x)e^{-\alpha_i(\lambda_i^2+l_i^2)(t-\xi)}T_{ii}(x,\xi)dxd\xi.$$

(3-43)

Substituting this expression into (3-27) yields the temperature distribution for region *i:*

$$T_i(x,t) = \sum_{m=1}^{\infty}\frac{\cos(\lambda_{im}x)}{N_m}\left\{\frac{q_o''\cos(\lambda_{im}L)}{k_i(\lambda_{im}^2 + l_i^2)}\left[e^{-\alpha_i(\lambda_{im}^2+l_i^2)(t-\tau)} - e^{-\alpha_i(\lambda_{im}^2+l_i^2)t}\right] + l_i^2\alpha_i\int_0^t\int_0^L \cos(\lambda_{im}x)e^{-\alpha_i(\lambda_{im}^2+l_i^2)(t-\xi)}T_{ii}(x,\xi)dxd\xi\right\}.$$

(3-44)

Specifically for the fiber and the matrix, equation (3-44) becomes

$$T_f(x,t) = \sum_{m=1}^{\infty}\frac{\cos(\lambda_{fm}x)}{N_m(\lambda_{fm})}\left\{\frac{q_o''\cos(\lambda_{fm}L)}{k_f(\lambda_{fm}^2 + l_f^2)}\left[e^{-\alpha_f(\lambda_{fm}^2+l_f^2)(t-\tau)} - e^{-\alpha_f(\lambda_{fm}^2+l_f^2)t}\right] + l_f^2\alpha_f\int_0^t\int_0^L \cos(\lambda_{fm}x)e^{-\alpha_f(\lambda_{fm}^2+l_f^2)(t-\xi)}T_m(x,\xi)dxd\xi\right\},$$

(3-45)

and

$$T_m(x,t) = \sum_{n=1}^{\infty}\frac{\cos(\lambda_{mn}x)}{N_n(\lambda_{mn})}\left\{\frac{q_o''\cos(\lambda_{mn}L)}{k_m(\lambda_{mn}^2 + l_m^2)}\left[e^{-\alpha_m(\lambda_{mn}^2+l_m^2)(t-\tau)} - e^{-\alpha_m(\lambda_{mn}^2+l_m^2)t}\right] + l_m^2\alpha_m\int_0^t\int_0^L \cos(\lambda_{mn}x)e^{-\alpha_m(\lambda_{mn}^2+l_m^2)(t-\xi)}T_f(x,\xi)dxd\xi\right\}.$$

(3-46)

Notice that these equations do not represent closed-form solutions for the temperature distribution in the fiber and in the matrix, since they are coupled. In order to obtain actual temperatures, these equations must be solved simultaneously. Because of the time integration, they are quite formidable mathematically and would require a great deal of computational capability.

3.2 Numerical Solution

As discussed above, equations (3-45) and (3-46) represent valid solutions for the temperature distribution in the fiber and in the matrix, but they are difficult to evaluate. In order to answer the question presented in Chapter 1, specific transient temperature distributions for the fiber and the matrix at the back face ($x = 0$) must be known. To obtain these a simple finite-difference model is considered in this section. In the finite-difference method the governing partial differential equation is discretized in space and in time to yield algebraic equations.

For the model used here, the number of axial and radial nodes remains arbitrary. This will allow for adjustments which will become necessary later on in the analysis. Figure 3-3 shows the details regarding the node distribution in the grid. Note that the spacing is uniform in each direction and within each phase, and that temperature variations in both the axial and the radial directions are considered.

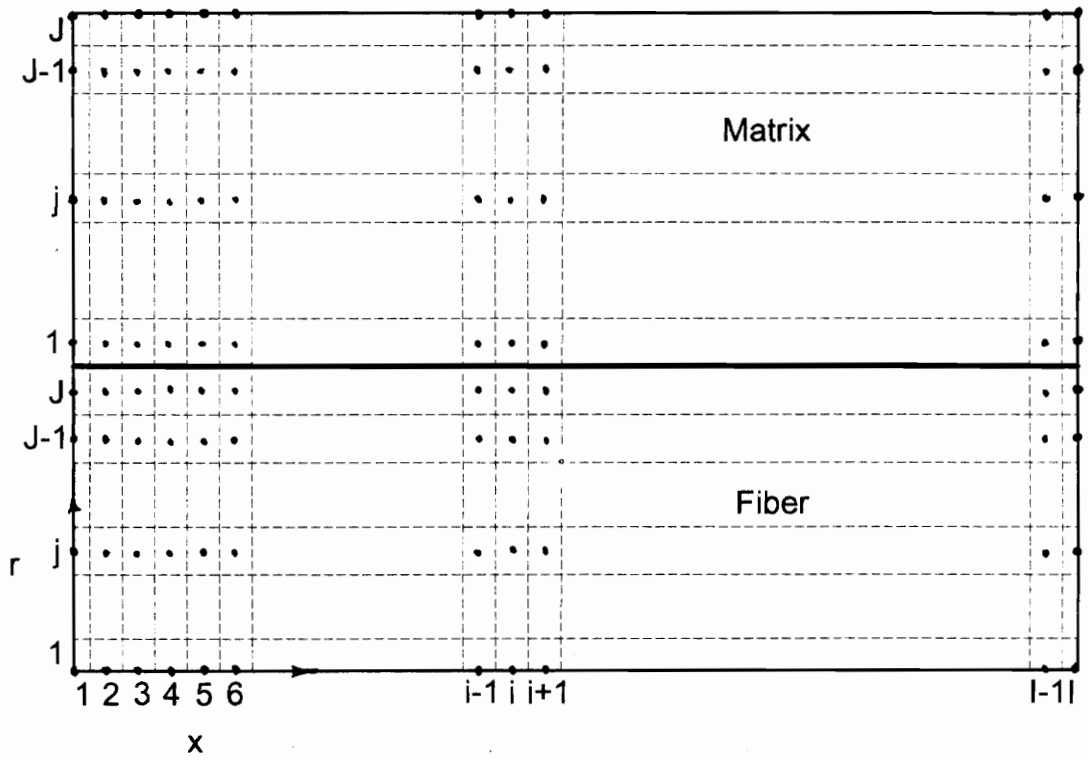

Figure 3-3 Control volume and node distribution in the fiber and matrix.

The method used for the derivation of the nodal equations is based on an energy balance. Furthermore, since a contact conductance between two materials with different properties is present, the concept of thermal resistance is also used. The finite-difference equations derived below are representative, and represent the building blocks for the model. Since the equations for the matrix and the fiber are very similar, the derivations shown here are restricted to the matrix only in order to avoid unnecessary repetition. Note that an implicit method is used with * denoting temperatures at the previous time step.

Matrix Equations

Node (*I, J*): Performing an energy balance around control volume (*I, J*) we get,

$$\sum_{l} q_{cond,l} + q(t) + q_{conv} = \dot{q}_{st}, \tag{3-47}$$

or using thermal resistance notation this can be written

$$\frac{T^m_{(I-1,J)} - T^m_{(I,J)}}{R^m_{x(J)}} + \frac{T^m_{(I,J-1)} - T^m_{(I,J)}}{2R^m_{r(J,J-1)}} + q''(t)A^m_J - hA^m_J T^m_{(I,J)} = \rho_m c_m \frac{\Delta x}{2} A^m_J \frac{T^m_{(I,J)} - T^{m\,*}_{(I,J)}}{\Delta t}, \tag{3-48}$$

where $R^m_{x(J)}$ is axial resistance to heat transfer, $R^m_{r(J,J-1)}$ is the radial resistance, A^m_J is the area normal to axial heat transfer, $q''(t)$ represents the energy coming from the laser pulse and h is the free convection coefficient. The superscript m refers to the matrix. The subscripts represent the node location, except in the resistances. For the axial resistance the subscripts denote the resistance between the nodes within each row, while for the radial resistance they represent the resistance between the nodes shown. For example

$R^m_{x(J)}$ is the axial resistance between the nodes in row J in the matrix, while $R^m_{r(J,J-1)}$ is the radial resistance between nodes i,J and i,J-1 in the matrix. The index i represent an arbitrary node in the axial direction with I representing the last axial node. Similarly, j represent an arbitrary node in the radial direction with J representing the last radial node.

Node (i, J): The energy balance around (i, J) is written

$$\sum_l q_{cond,l} = \dot{q}_{st}, \tag{3-49}$$

or,

$$\frac{T^m_{(i-1,J)} - T^m_{(i,J)}}{R^m_{x(J)}} + \frac{T^m_{(i+1,J)} - T^m_{(i,J)}}{R^m_{x(J)}} + \frac{T^m_{(i,J-1)} - T^m_{(i,J)}}{R^m_{r(J,J-1)}} = \rho_m c_m \Delta x A^m_J \frac{T^m_{(i,J)} - T^{m\,*}_{(i,J)}}{\Delta t}. \tag{3-50}$$

Node (i, j): As before, an energy balance yields

$$\frac{T^m_{(i-1,j)} - T^m_{(i,j)}}{R^m_{x(j)}} + \frac{T^m_{(i+1,j)} - T^m_{(i,j)}}{R^m_{x(j)}} + \frac{T^m_{(i,j-1)} - T^m_{(i,j)}}{R^m_{r(j,j-1)}} + \frac{T^m_{(i,j+1)} - T^m_{(i,j)}}{R^m_{r(j,j+1)}} = \rho_m c_m \Delta x A^m_j \frac{T^m_{(i,j)} - T^{m\,*}_{(i,j)}}{\Delta t}. \tag{3-51}$$

Node (I, j): An energy balance around this nodes gives

$$\sum_l q_{cond,l} + q(t) + q_{cnv} = \dot{q}_{st}, \tag{3-52}$$

or,

$$\frac{T^m_{(I-1,j)} - T^m_{(I,j)}}{R^m_{x(j)}} + \frac{T^m_{(I,j-1)} - T^m_{(I,j)}}{2R^m_{r(j,j-1)}} + \frac{T^m_{(I,j+1)} - T^m_{(I,j)}}{2R^m_{r(j,j+1)}} + q''(t)A^m_j - hA^m_j T^m_{(I,j)} = \rho_m c_m \frac{\Delta x}{2} A^m_j \frac{T^m_{(I,j)} - T^{m\ *}_{(I,j)}}{\Delta t}.$$

(3-53)

Node (i, 1): Around this node the contribution from the fiber becomes important. The energy balance is

$$\sum_l q_{cond,l} = \dot{q}_{st}, \tag{3-54}$$

or,

$$\frac{T^m_{(i-1,1)} - T^m_{(i,1)}}{R^m_{x(1)}} + \frac{T^m_{(i+1,1)} - T^m_{(i,1)}}{R^m_{x(1)}} + \frac{T^f_{(i,J)} - T^m_{(i,1)}}{R_{\text{int}}} + \frac{T^m_{(i,2)} - T^m_{(i,1)}}{R^m_{r(1,2)}} = \rho_m c_m \Delta x A^m_1 \frac{T^m_{(i,1)} - T^{m\ *}_{(i,1)}}{\Delta t}. \tag{3-55}$$

In the equations shown above, $R^m_{x(j)} = \dfrac{\Delta x}{A^m_j k_m}$, $R^m_{r(j,j+1)} = \dfrac{\ln(r^m_{j+1}/r^m_j)}{\theta k_m \Delta x}$, $R_{\text{int}} = \dfrac{\ln(r^m_1/a)}{\theta k_m \Delta x} + \dfrac{1}{h_c \theta a \Delta x} + \dfrac{\ln(a/r^f_1)}{\theta k_f \Delta x}$, where r^m_j and r^f_j refer to the radial node location in the matrix and fiber respectively.

The listing of the FORTRAN program used to solve the finite-difference equations is included in the Appendix.

CHAPTER 4

4.1 Composite to be Analyzed

The parameters used for the evaluation of the back face temperatures presented in the next section are based on the dimensions and properties of the samples used by Hasselman et al. [26] in an experiment done to determine thermal properties. The following list summarizes this information:

Fibers:
Radius = a = 5 μm
Thermal conductivity = k_f = 100 W/m K
Density = ρ_f = 2000 kg/m^3
Thermal capacity = c_f = 717 J/kg K
Length = L = 2 mm

Matrix:
Outer radius = $b = 5\sqrt{2}$ μm
Thermal conductivity = k_m = 1 W/m K
Density = ρ_m = 2160 kg/m^3
Thermal capacity = c_m = 766 J/kg K
Length = L = 2 mm

Since the experiment described in [26] was conducted in a near-vacuum of 0.13 Pa, the convective heat transfer coefficient will be assumed to be negligible for the purpose of this work. It follows that since no dissipation of heat is possible, an equilibrium temperature in the composite will be reached after the energy pulse is

deposited in the sample and the transients have passed[1]. We can estimate this equilibrium temperature by using a simple thermodynamic argument. The energy stored in a body can be written

$$E_{st} = mcT_{eq}, \tag{4-1}$$

where m is the mass, c is the heat capacity, and T_{eq} is the equilibrium temperature. For the composite being considered in this study we can rewrite equation (4-1) as

$$q_o{}''\,\tau\pi b^2 = L\left[\rho_f c_f \pi a^2 + \rho_m c_m \pi (b^2 - a^2)\right] T_{eq}, \tag{4-2}$$

or

$$T_{eq} = \frac{q_o{}''\,\tau b^2}{L\left[\rho_f c_f a^2 + \rho_m c_m (b^2 - a^2)\right]}. \tag{4-3}$$

But since $b^2 = 2a^2$, it follows that

$$T_{eq} = \frac{2q_o{}''\,\tau}{L\left[\rho_f c_f + \rho_m c_m\right]}, \tag{4-4}$$

where τ is the energy pulse duration and $q_o{}''$ is the heat flux of the laser pulse. The following values will be used in the next section for the purpose of numerical calculations: $\tau = 0.5$ ms and $q_o{}'' = 20\times10^6$ W/m^2. Equation (4-3) can also be derived by considering the one-dimensional radial version of problem (2-1)-(2-3) with all boundaries insulated and internal heat generation $q_o{}''/L$ for $t < \tau$. Since all boundaries are of the second kind, the

[1]Radiation losses may become significant, especially for low values of thermal conductivity, but they will be neglected here since the time scale of the experiment is so small.

eigenvalue $\lambda_0 = 0$ is also a part of the solution. The term in the series solution corresponding to this eigenvalue represents the equilibrium temperature after all the transients have passed and is identical to equation (4-3).

The thermal properties for the composite can be estimated by measuring the time it takes for the back face to reach one-half ($t_{1/2}$) the equilibrium temperature, T_{eq}. If no energy dissipation is possible and if the duration of the energy pulse τ is small compared to the time scale of the experiment then equation (1-2) applies and

$$\alpha_e = 1.38\frac{L^2}{\pi^2 t_{1/2}}, \tag{4-5}$$

where α_e is the equivalent thermal diffusivity for the composite. Equation (4-5) assumes homogeneity and is valid if the criteria proposed by Taylor et al [24] and Balageas et al. [25] discussed in Chapter 1 apply. Furthermore, under these conditions we can also write

$$\alpha_e = \frac{k_e}{\rho_f c_f v_f + \rho_m c_m v_m}, \tag{4-6}$$

where k_e is the equivalent thermal conductivity and v refers to the phase volume fractions. It follows that

$$k_e = 1.38\frac{L^2}{\pi^2 t_{1/2}}(\rho_f c_f v_f + \rho_m c_m v_m). \tag{4-7}$$

In the next section we use equation (4-7) to estimate the equivalent thermal conductivity of the composite introduced in Section 4.1, and compare the results with the experimental values found by Hasselman et al. in [26].

4.2 Back Face Temperature Profiles

In this section we present the back face temperature profiles in graphical form using the results from the FORTRAN program included in the Appendix. Recall that the number of nodes in the radial and axial directions are yet to be determined. In order to do this we use a limiting case for equations (3-45) and (3-46). If we let h_c = 0 (no thermal contact between the fibers and the matrix) in these equations, the terms containing the spatial and time integral vanish, and these expressions become closed-form solutions. Now that an exact analytical solution is available, the number of axial nodes in the finite-difference solution can be varied to yield results that match those of the exact solution[2]. It follows that 400 nodes in the axial direction are needed to approximate the temperature fields produced by the exact solution. The number of radial nodes is not as critical because the gradients in this direction are insignificant compared to those in the axial direction. Based on this, only one node within each phase is necessary to produce accurate results[3]. Figures 4-1 and 4-2 show the temperature distribution at the back face and at the front face for this limiting case.

It is important to note how much faster the response for the fiber is compared to that of the matrix. Since the fiber and the matrix are thermally uncoupled for $h_c = 0$, equation (4-4) does not apply, and two different equilibrium temperatures are reached. These are given by:

$$T_{eq,i} = \frac{q_o'' \tau}{L \rho_i c_i}. \qquad (4\text{-}8)$$

[2]A listing of the Fortran program used to calculate the eigenvalues and evaluate the infinite series for this special case is included in the Appendix.

[3]Temperature fields were obtained for different values of h_c and for higher number of radial nodes, but the radial temperature gradients were insignificantly small.

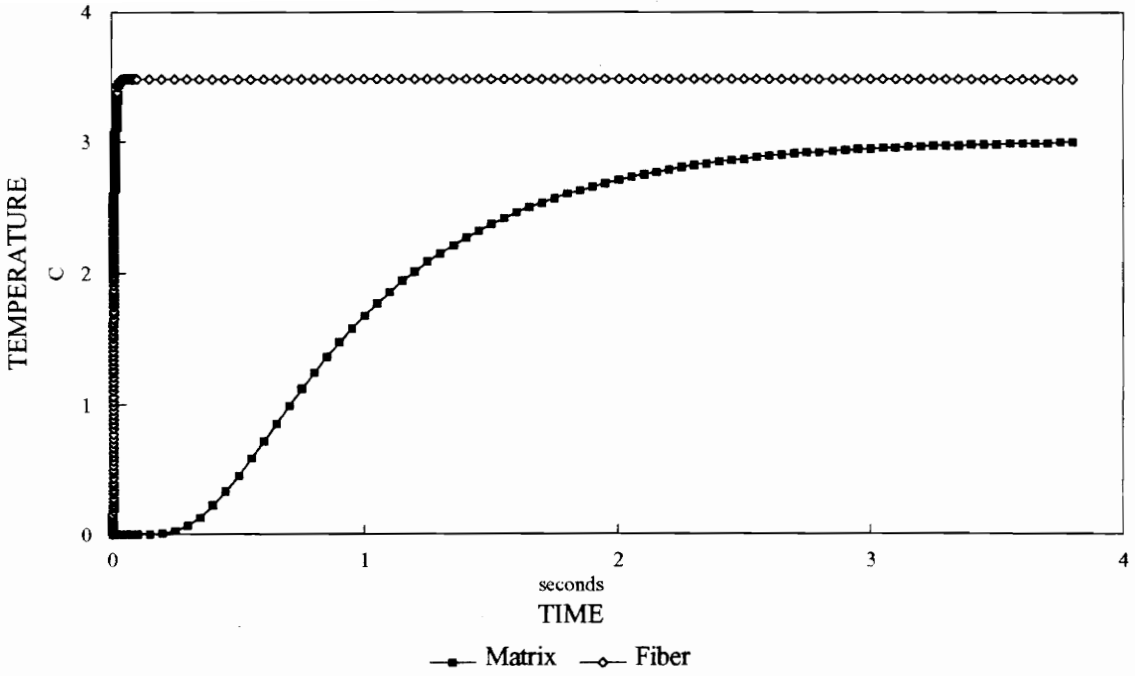

Figure 4-1 Back face temperature rise as a function of time for $h_c = 0$.

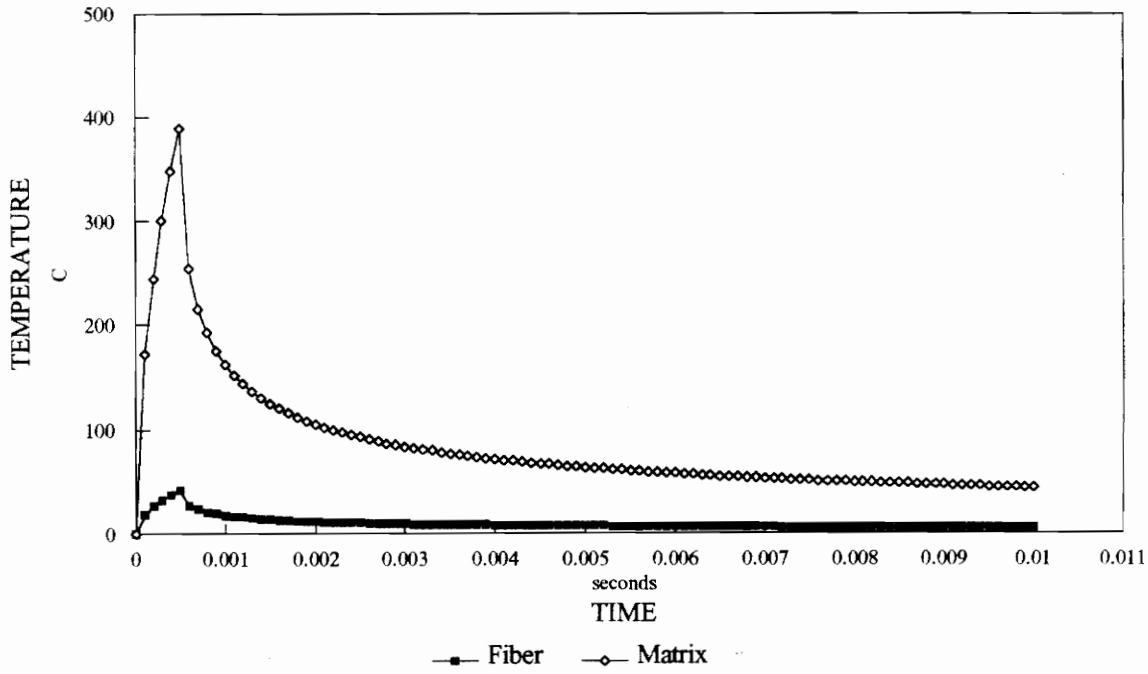

Figure 4-2 Front face temperature as a function of time for $h_c = 0$.

By using the parameters presented in Section 4.1, it follows that $T_{eq,f} = 3.49^0\text{C}$ and $T_{eq,m} = 3.02^0\text{C}$ above the ambient temperature T_∞.

Next we consider the temperature response at the back face and at the front face of the composite for perfect thermal contact or $h_c = \infty$. Figure 4-3 shows the temperature rise at the back face for the matrix and for the fiber. As expected for perfect thermal contact, the temperature response is exactly the same for both phases. This renders the composite homogeneous as far as the flash method is concerned and the equations presented above apply. Using equation (4-4) and the properties listed in Section 4.1, it follows that the equilibrium temperature above the ambient temperature T_∞ should be

$$T_{eq} = \frac{2(20\times10^6\text{W/m}^2)(.0005\text{s})}{(.002\text{m})\left[(2000\text{kg/m}^3)(717\text{J/kg}^0\text{C})+(2160\text{kg/m}^3)(766\text{J/kg}^0\text{C})\right]} = 3.24^0\text{C}$$

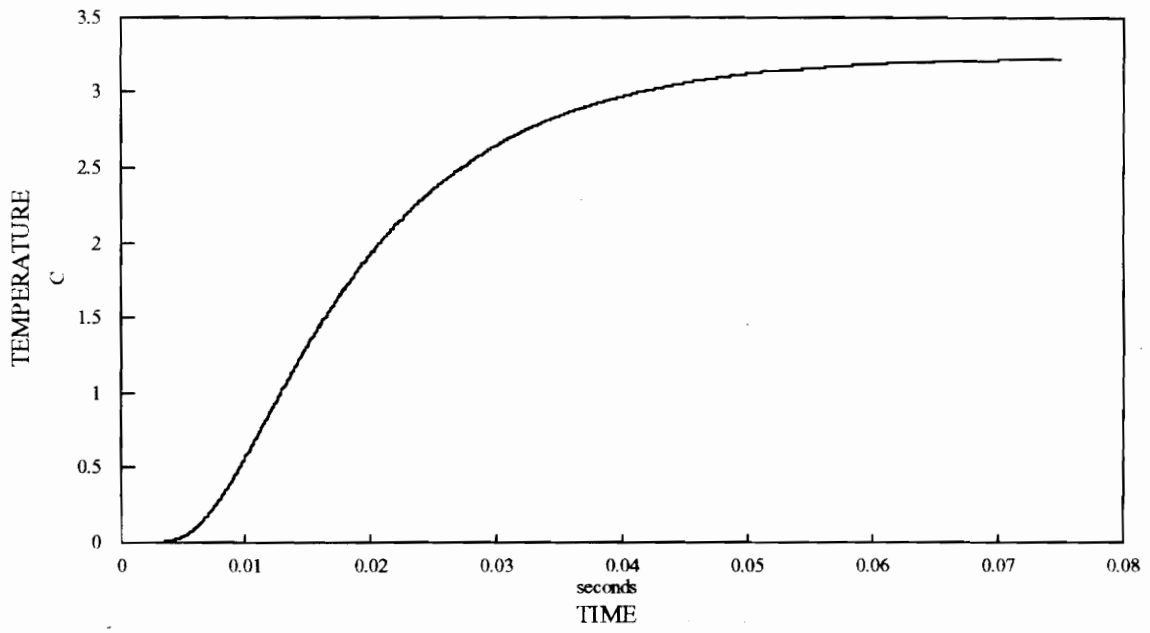

Figure 4-3 Back face temperature rise as a function of time for $h_c = \infty$.

This value agrees very well with the asymptotic temperature shown in Figure 4-3. Now we can estimate the equivalent thermal conductivity of the composite using equation(4-7). From Figure 4-3 it follows that $t_{1/2}$ =.0170s, and

$$k_e = 1.38\frac{(.002\text{m})^2}{2\pi^2(.0170\text{s})}\left[(2000\text{kg/m}^3)(717\text{J/kg°C}) + (2160\text{kg/m}^3)(766\text{J/kg°C})\right] = 51.1\ \text{W/m K}.$$

This value is within 10% of the reported experimental value of 56.3 W/m K presented in [26]. The discrepancy may be explained by recalling that equation (4-7) was derived assuming that the energy is deposited in the material instantaneously. Mathematically this is represented by the delta function, $\delta(t)$. If the energy pulse is characterized by the delta function, then the heat front can start propagating down to the back face faster than we have assumed here. It follows that $t_{1/2}$ would occur at a lower time, and because $k_e \propto \frac{1}{t_{1/2}}$, the value for k_e would increase, more closely matching the experimental results. It is difficult to simulate the effect of a delta function in a numerical analysis. Here we let the energy pulse last τ = 0.5 ms, which is 34 times smaller than the value of $t_{1/2}$. However, the delta function assumes that all the energy is deposited instantaneously, yielding a τ which is infinitely smaller than $t_{1/2}$. We could reconcile the discrepancy between the experimental and numerical values by applying the finite pulse time corrections presented by Taylor and Clark [34]. However, since we are only interested in the role of the contact conductance term, we will not present these corrections here .

The front face transient temperature response is shown in Figure 4-4. The very sharp peaks are caused by the high concentration of energy in the front face during the irradiation of the laser. Notice that the matrix reaches a higher maximum temperature than the fiber because of its poorer conductivity. After the energy source is turned off, the

fiber and matrix temperature merge quickly, making the radial temperature distribution uniform.

Now we try to answer the question that motivated this work: Assuming a high fiber volume fraction and a high axial-to-radial fiber dimension ratio, how small can the contact resistance between the fiber and the matrix be before radial thermal homogeneity is no longer valid? In order to address this question we will show several graphs that show the back face temperature rise for decreasing values of h_c.

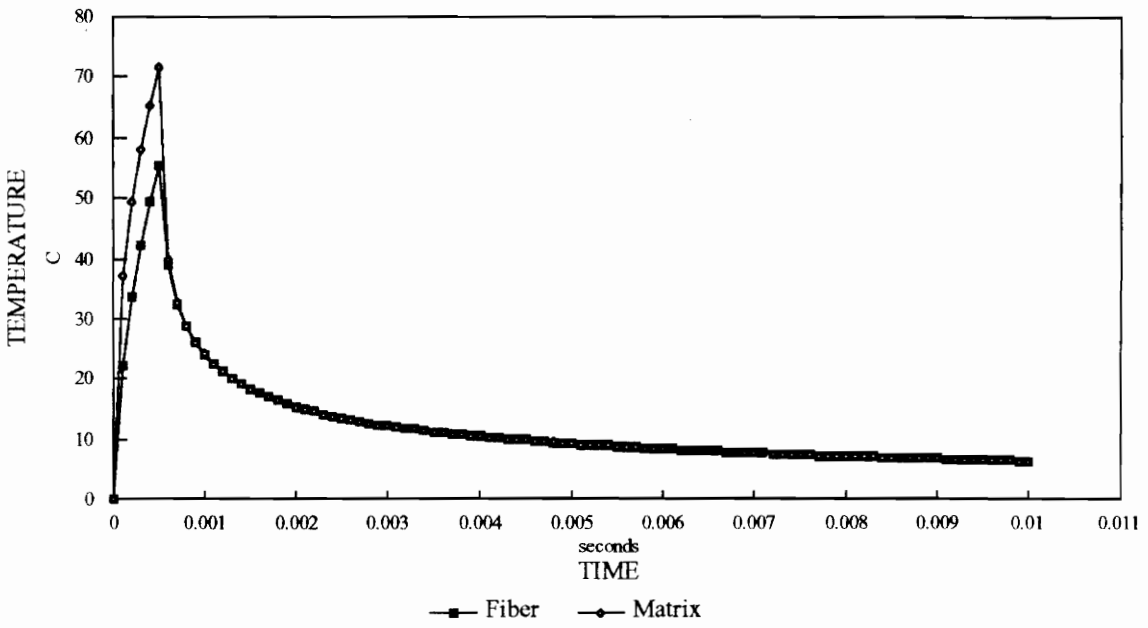

Figure 4-4 Front face temperature as a function of time for $h_c = \infty$.

We start by presenting the temperature response for $h_c = 10^5$ W / m^{2}K. Figure 4-5 shows the temperature rise at the back face. This graph is identical to the one shown in Figure 4-3, yielding the same $t_{1/2}$ and k_e. This means that, for the back face, $h_c = 10^5$ W / m^{2}K can be considered to be perfect thermal contact, and thermal homogeneity is achieved for this value of thermal conductance.

Figure 4-6 shows the response at the front face. This plot reveals the only significant difference between perfect thermal contact and $h_c = 10^5$ W / m^{2}K: the marked contrast between the maximum temperatures in the fiber and in the matrix. For this value of thermal contact, the maximum temperature in the matrix is almost three times higher than that of the fiber. However, the temperatures for the fiber and matrix at the front face do merge quickly after the energy source is turned off, establishing radial thermal equilibrium and a uniform heat front.

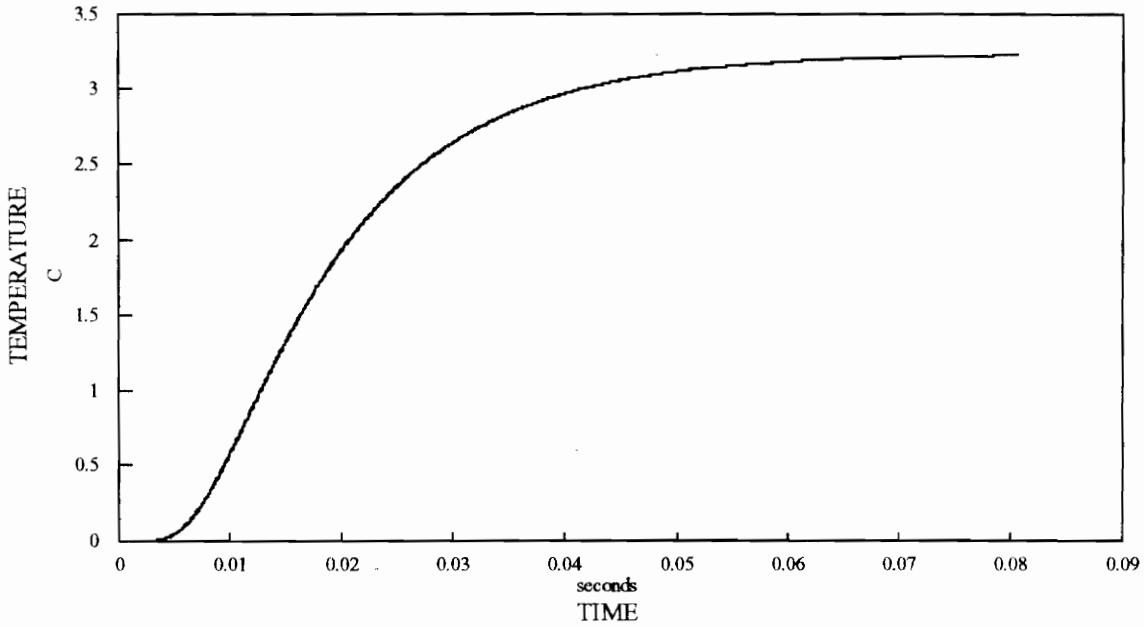

Figure 4-5 Back face temperature rise as a function of time for $h_c = 10^5$ W / m^{2}K.

The back face temperature plot for $h_c = 10^4$ W / m^{2}K, shown in Figure 4-7, starts to show signs of thermal uncoupling between the fiber and the matrix. However, the differences are barely noticeable. Considering that real world instruments may not be able to account for this minute temperature difference, it is safe to assume that thermal homogeneity still holds for this value of thermal conductance. The effective thermal

conductivity calculated using these data is within 2% of the value obtained under perfect thermal contact. We will use this deviation as the criterion for establishing homogeneity.

The maximum temperature differences start to become large for this relatively low value of thermal contact as shown in Figure 4-8. As before the heat front in the front face becomes uniform after the energy pulse is deposited in the sample, but only after two $t_{1/2}$'s have passed. For the two previous cases the front face temperatures merge much faster (less than $1/2t_{1/2}$ for the worst case).

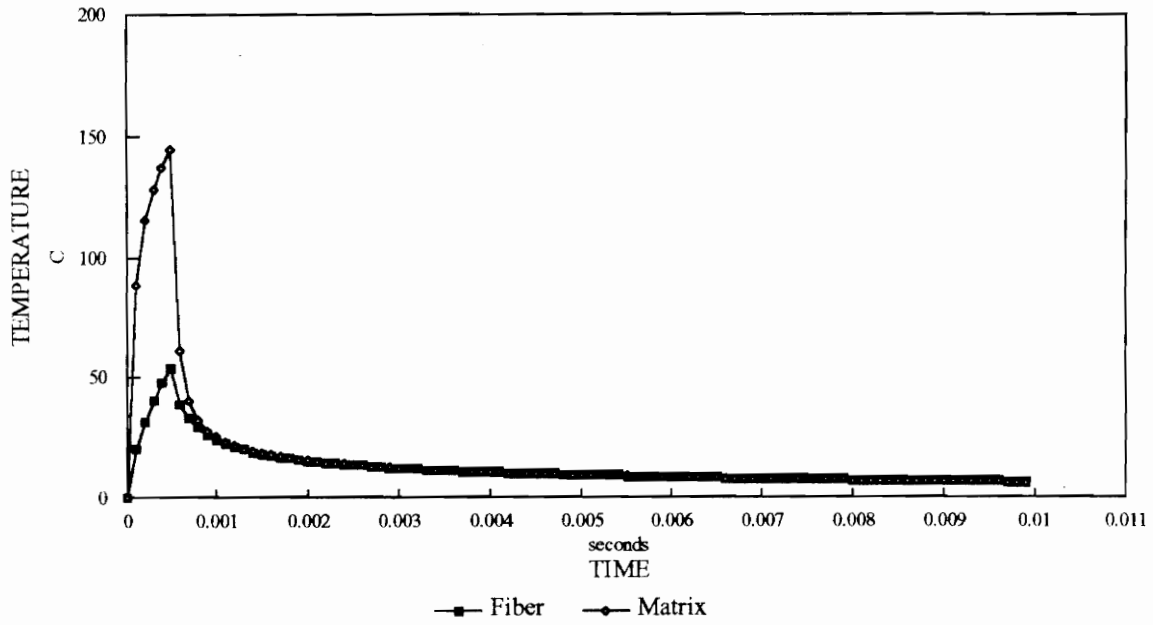

Figure 4-6 Front face temperature as a function of time for $h_c = 10^5$ W / m^{2}K.

Many of the trends observed for $h_c = 10^4$ W / m^{2}K are also present, but to a greater extent, for the case $h_c = 5000$ W / m^{2}K as shown in Figure 4-9. Here the uncoupling of the back face temperature fronts become more discernible, with the matrix temperature rise lagging that of the fiber. If Figure 4-9 is used to estimate $t_{1/2}$, we find

that the calculated value for k_e is about 10% lower than the one calculated assuming perfect thermal contact.

Figure 4-10 shows what the response at the back face may look like if the coupling between the matrix and the fibers is poor (for example $h_c = 100 \mathrm{W/m^2K}$). Under this condition the back face matrix temperature lags that of the fiber by a considerable margin during most of the rise. Obviously for this case the concept of homogeneity does not apply at all and equivalent thermal properties cannot be determined from experimental data acquired using the flash-method. It is important to point out that the temperature sensing equipment used in experiments cannot distinguish between the temperature rise of the fiber or that of the matrix. It can only record the back face average temperature, and for the case being considered the average temperature yields ambiguous results

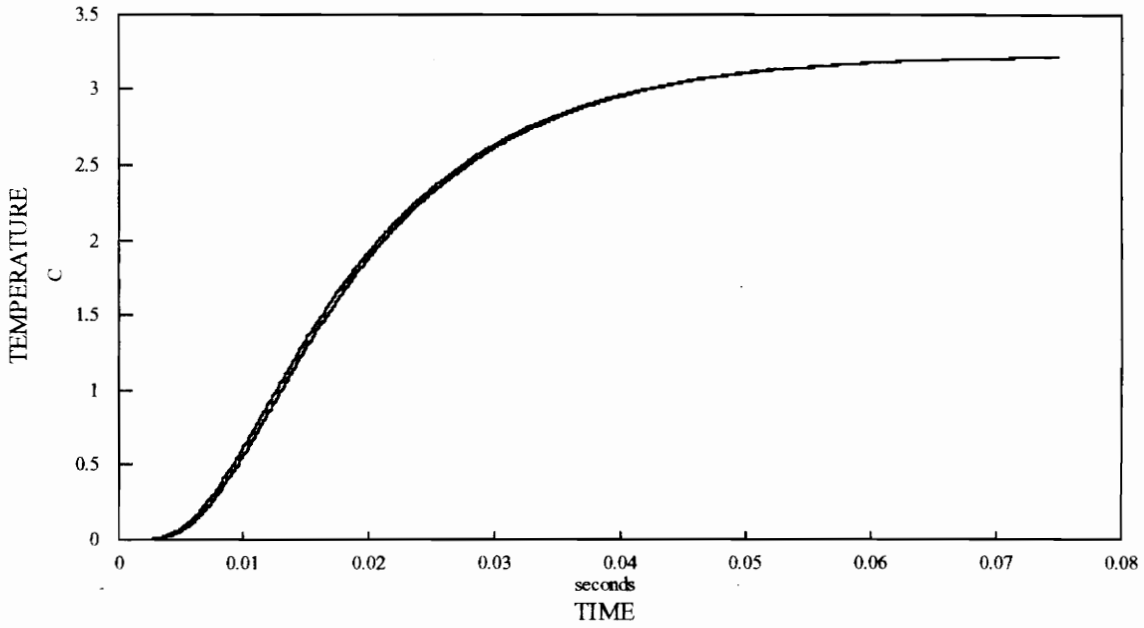

Figure 4-7 Back face temperature rise as a function of time for $h_c = 10^4 \ \mathrm{W/m^2K}$.

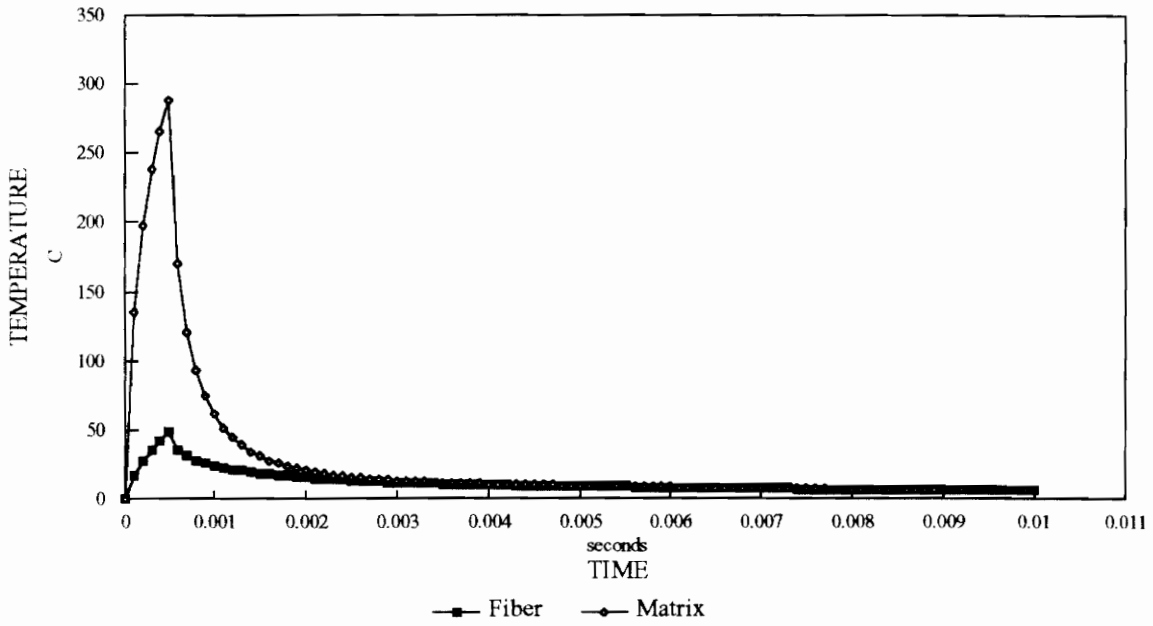

Figure 4-8 Front face temperature as a function of time for $h_c = 10^4$ W / m^{2}K.

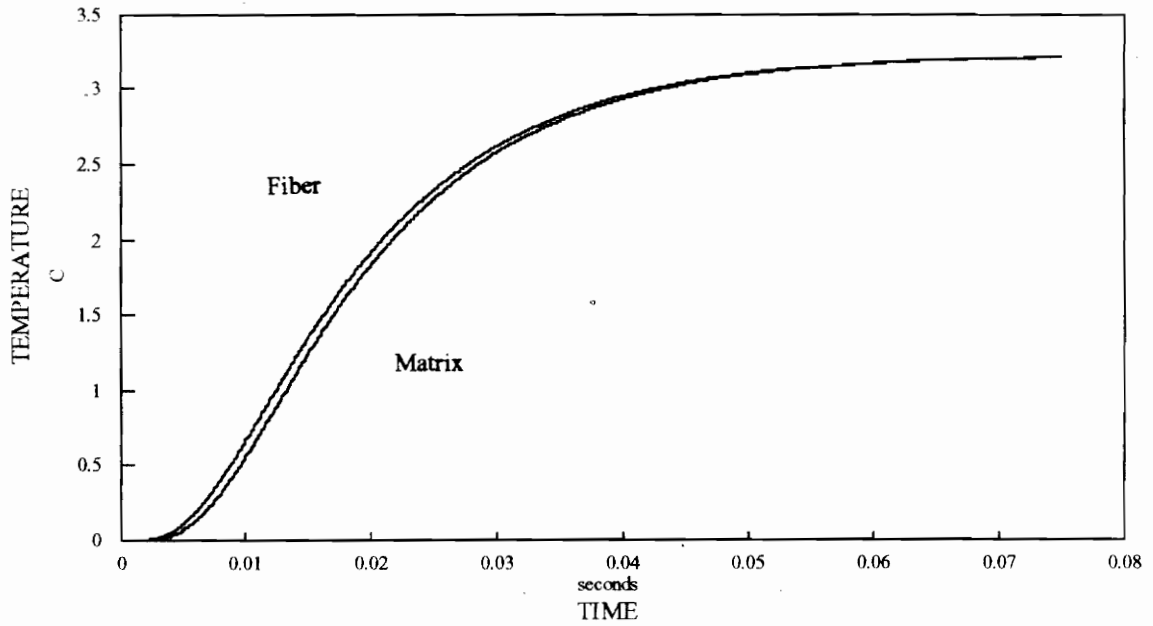

Figure 4-9 Back face temperature rise as a function of time for h_c = 5000 W / m^{2}K.

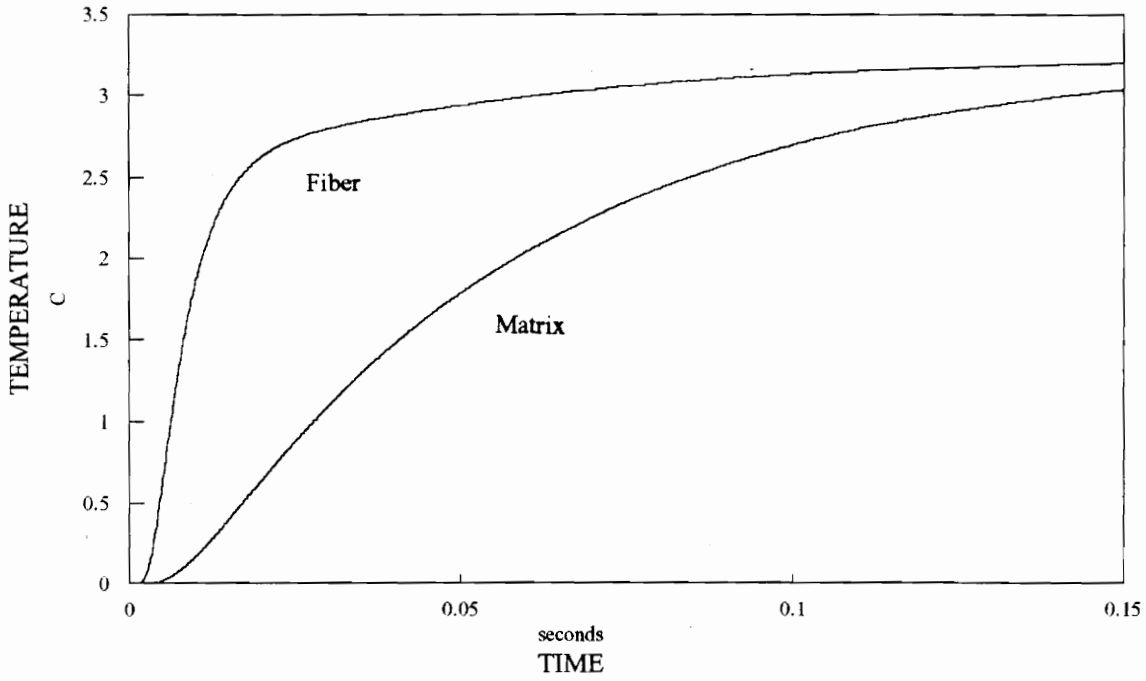

Figure 4-10 Back face temperature rise as a function of time for $h_c = 100\ \mathrm{W/m^2K}$.

4.3 A General Criterion

Some readers may be concerned by the fact that the discussion presented in the previous section was restricted to a specific type of composite and does not apply generally. This is a valid concern which will be addressed in this section. However, the dimensions used above are typical for most composites subject to the flash method experiment so we will not consider the effect of changing them here. In other words, the first two criteria for homogeneity presented in Chapter 1 are met: the fiber fraction in the composite must be high (i.e., $\geq$ 50%), and the axial dimension must be much greater than the radial dimension (i.e., $L/a > 100$).

The parameters which are most likely to be different from the case presented above are the thermal conductivities of the individual phases. The heat capacity term ($\rho_i c_i$) does not vary much from material to material. Indeed this is the case for the fiber and matrix presented above. Even though the thermal conductivities differ by two orders of magnitude, the heat capacities are within 14% of each other.

We have already established that for a fiber-to-matrix thermal conductivity ratio of 100, the lowest contact conductance value allowed for homogeneity is about 10,000 W/m^{2}K. If the fiber-to-matrix conductivity ratio goes up, qualitatively we expect the minimum value of the contact conductance term to increase. The converse is also true: if the fiber-to-matrix ratio is reduced, then $h_{c,\min}$ goes down.

Consider the case for which there is no thermal contact between the two phases. As the thermal conductivities of the fiber and the matrix approach each other the axial temperature fronts diffuse at rates that approach each other accordingly. If the energy fronts diffuse at similar rates then thermal homogeneity is established without the need for thermal contact.

As the thermal conductivities become different the heat fronts diffuse at different rates. In this case thermal homogeneity can only be established if a sufficiently high

thermal contact is present to allow for the exchange of energy between the phases and, therefore, the creation of a uniform temperature front.

In order to test the qualitative reasoning presented above, the effect of changing the thermal conductivity ratio was investigated quantitatively; initially the results were surprising. For example, if we keep the previous value of k_f = 100 W/mK and make k_m = 10 W/mK (thermal conductivity ratio of 10 to 1), the result obtained for $h_{c,\min}$ are not very different from those observed for the original case (thermal conductivity ratio of 100 to 1). Specifically, $h_{c,\min}$ dropped (as expected from the argument presented above) from 10,000 W/m^{2}K to about 9,100 W/m^{2}K. So, even though the thermal conductivity ratio was increased by a factor of 10, $h_{c,\min}$ was only reduced by 9%. However, when the thermal conductivity ratio was increased to 1000 to 1, $h_{c,\min}$ increased tenfold. Apparently this system is rather insensitive to matrix thermal conductivity variations, but is a strong function of the fiber thermal conductivity. This observation can be explained by analyzing the resistance network representation of the composite shown in Figure 4-11. The development presented below is analogous to the derivation of the Biot number in transient heat conduction.

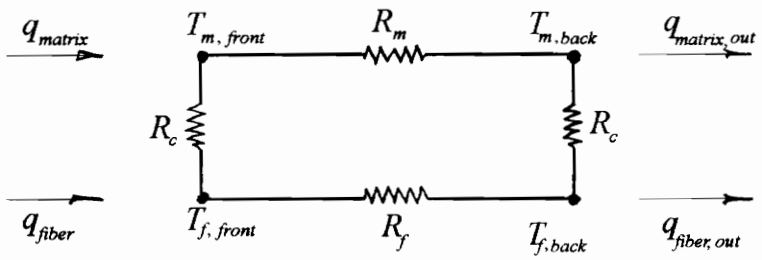

Figure 4-11 Approximate network representation of fiber-reinforced composite.

Assuming $k_f > k_m$ and steady-state conditions we can write

$$q_{fiber,out} = \frac{T_{f,front} - T_{f,back}}{R_f} - \frac{T_{f,back} - T_{m,back}}{R_c}, \qquad (4\text{-}9)$$

and

$$q_{matrix,out} = \frac{T_{m,front} - T_{m,back}}{R_m} + \frac{T_{f,back} - T_{m,back}}{R_c}. \tag{4-10}$$

For thermal homogeneity at the back face it follows that

$$q''_{fiber,out} = \frac{q_{fiber,out}}{A_f} \approx \frac{q_{matrix,out}}{A_m} = q''_{matrix,out}, \tag{4-11}$$

or

$$\frac{1}{A_f}\left[\frac{T_{f,front} - T_{f,back}}{R_f} - \frac{T_{f,back} - T_{m,back}}{R_c}\right] \approx \frac{1}{A_m}\left[\frac{T_{m,front} - T_{m,back}}{R_m} + \frac{T_{f,back} - T_{m,back}}{R_c}\right]. \tag{4-12}$$

Using $R_f = \frac{L}{A_f k_f}$, $R_m = \frac{L}{A_m k_m}$, and $R_c = \frac{1}{A_c h_c}$, equation (4-12) becomes

$$k_f \frac{T_{f,front} - T_{f,back}}{L} - h_c \frac{A_c}{A_f}\left(T_{f,back} - T_{m,back}\right) \approx k_m \frac{T_{m,front} - T_{m,back}}{L} + h_c \frac{A_c}{A_m}\left(T_{f,back} - T_{m,back}\right). \tag{4-13}$$

Rearranging equation (4-13) we get

$$\frac{k_f}{L}\left(\frac{T_{f,front} - T_{f,back}}{T_{m,front} - T_{m,back}}\right) \approx \frac{k_m}{L} + h_c A_c \left(\frac{1}{A_m} + \frac{1}{A_f}\right)\left(\frac{T_{f,back} - T_{m,back}}{T_{m,front} - T_{m,back}}\right). \tag{4-14}$$

For thermal homogeneity at the back face, $\frac{T_{f,front} - T_{f,back}}{T_{m,front} - T_{m,back}} \approx 1$, and $\frac{T_{f,back} - T_{m,back}}{T_{m,front} - T_{m,back}} =$ small

so we can rewrite equation (4-14) as

$$\frac{k_f - k_m}{Lh_c A_c} \frac{1}{\left(\frac{1}{A_m} + \frac{1}{A_f}\right)} = \text{small}. \tag{4-15}$$

Now we introduce the expressions for the areas using $A_f = \pi a^2$, $A_m = \pi\left(b^2 - a^2\right)$ and $A_c = \pi aL$ to get

$$\frac{k_f - k_m}{L^2 h_c} a\left[1 - \left(\frac{a}{b}\right)^2\right] = \text{small}. \tag{4-16}$$

From the results presented in the previous section it follows that homogeneity will be achieved at the back face if

$$h_c \geq 161.6 \frac{k_f - k_m}{L^2} a\left[1 - \left(\frac{a}{b}\right)^2\right]. \tag{4-17}$$

The constant on the right hand side is, to an extent, arbitrary. It was chosen so that the average back face temperature at $t_{1/2}$ (for the case study presented in Section 4.2) is within 2% of the average back face temperature at $t_{1/2}$ for perfect thermal contact. Note that this inequality correctly predicts that for $k_f = k_m$ (a homogeneous material) no thermal contact is required between the phases to achieve homogeneity at the back face. It also predicts that $h_{c,\min} \to 0$ as $a \to b$ which is what we would expect qualitatively.

Now the quantitative observations presented above are easily explained. For the composite under consideration $b^2 = 2a^2$, so equation (4-17) reduces to

$$h_{c,\min} \geq 80.81 \frac{a}{L^2}\left(k_f - k_m\right).$$

If $k_f >> k_m$, k_f dominates the equation and $h_{c,\min}$ becomes approximately directly proportional to k_f, and nearly unaffected by changes in k_m. As the thermal conductivity ratio (k_f / k_m) approaches unity, the thermal contact required for homogeneity decreases and both k_f and k_m become significant terms in the equation.

The predictions made by equation (4-17) for different values of k_f and k_m were tested using the computer program included in the Appendix. For example, it was found that for a composite with k_f= 1000 W/mK and k_m= 0.1 W/mK, the predicted minimum contact conductance yielded results at $t_{1/2}$ that were within 2% the results obtained using perfect thermal contact. Clearly this composite represents a 'worst case scenario' with conductivities between the phases differing by four orders of magnitude, yet the prediction for $h_{c,\min}$ is excellent. Other predictions made by (4-17) using different values of thermal conductivities were as good or better than the one for the 'worst case scenario' presented above. Clearly equation (4-17) is quite effective in predicting the minimum value of thermal contact which will yield homogeneous temperature fronts at the back face of fiber-reinforced composite samples subject to the flash method.

4.4 Summary and Conclusions

The flash method proposed by Parker in the early sixties is one of the most important experimental procedures to determine the thermal properties of homogeneous materials. Because of the versatility of this method, researchers have attempted to extend its usefulness into the realm of composite material. However, some difficulties arise because of the existence of preferential heat paths in heterogeneous materials, such as fiber-reinforced composites. For the flash method to yield meaningful results when applied to these type of composites, a homogeneous temperature front must exist at the back face of the sample, where the measurements are made. According to the literature three conditions must be met for this to occur:

1. the fiber-to-matrix volume ratio must be greater than 50% (i.e., $a^2 \geq 2b^2$):
2. the axial dimension of the sample must be much larger than the radii of the fibers (i.e., $L/a > 100$);
3. the thermal contact between the fibers and the matrix must be high.

Since most fiber-reinforced composite samples used in flash method experiments meet the first two criteria presented above, attention was focused on the contact conductance term. In order to analyze the role of this term a mathematical model consisting of a cylindrical fiber surrounded by a matrix shell was used. Two popular analytical methods were used to try to solve the governing equations, but because of mathematical difficulties closed-form solutions were impossible to obtain. Therefore, a finite-difference scheme was used to obtain the temperature responses. It was found that in order for a fiber-reinforced composite to achieve thermal homogeneity at the back face, the inequality

$$h_c \geq 161.6 \frac{k_f - k_m}{L^2} a \left[1 - \left(\frac{a}{b} \right)^2 \right]$$

must be satisfied, along with criteria 1. and 2. presented above.

REFERENCES

[1] H. M. Burte and A. Lawley, "Composite Material", pp 225-232 in *McGraw-Hill Encylopedia of Science and Technology*, vol. **4**, McGraw-Hill, New York (1992).

[2] H. S. Carslaw and J. C. Jaeger, *Conduction of Heat in Solids.* 2nd ed., pp 305-347, Clarendon Press, Oxford (1959).

[3] V. Vodicka, "Eindimensionale Waermeleitung in geschichteten Koerpern", *Mathematische Nachrichten,* **14** (1955).

[4] V. Vodicka, "Waermeleitung in geschichteten Kugel-und Zylinderkoerpern", *Schweizer Archiv,* **10** (1950).

[5] P. E. Bulavin and V. M. Kascheev, "Solution of the Nonhomogeneous Conduction Equation for Multilayered Bodies", *Int. J. Chem. Engng.*, **5**, 112-115 (1965).

[6] H. L. Beach, "The Application of the Orthogonal Expansion Technique to Conduction Heat Transfer Problems in Multilayer Cylinders", M.S. Thesis Mechanical and Aerospace Engineering, North Carolina State University, Raleigh, North Carolina, (1967).

[7] C. J. Moore, "Heat Transfer Across Surfaces in Contact and Studies of Transients in One-dimensional Composite Systems", Ph.D. Thesis, Mechanical Engineering Department, Southern Methodist University, Dallas, Texas, (1967).

[8] G. P. Mulholland and M. H. Cobble, "Diffusion Through Composite Media", *Int. J. Heat Mass Trans.*, **15**, 147-160 (1972).

[9] J. Padovan, "Solution of Transient Temperature Fields in Laminated Anisotropic Slabs and Cylinders", *J. Engng. Sci.*, **13**, 247-260 (1975).

[10] J. Baker-Jarvis and R. Inguva, "Heat Conduction in Layered, Composite Materials", *J. Appl. Phys.*, **57**, 1569-1573 (1985).

[11] H. J. Choi and S. Thangjitham, "Heat Conduction in Laminated Anisotropic Composites with a Debonding", *Int. J. Engng. Sci.*, 7, 819-829, (1991).

[12] J. I. Frankel, B. Vick and M. N. Ozisik, "General Formulation and Analysis of Hyperbolic Heat Conduction in Composite Media", *Int. J. Heat Mass Trans.*, **30**, 1293-1305, (1987).

[13] A. Haji-Sheikh, "Heat Diffusion in Heterogeneous Bodies Using Heat-Flux-Conserving Basis Functions", *J. Heat Trans.*, **110**, 276-282, (1988).

[14] F. Gordaninejad, "Enhancement of Thermal Conductivities in Polymeric Fiber Reinforced Composite Materilas", *J. Engng. Mat. Tech.*, **114**, 416-421, (1992).

[15] B. W. James, G. H. Wostenholm, G. S. Keen, S. D. McIvor, "Prediction and Measurement of the Thermal Conductivity of Composite Materials", *J. Phys. D:Appl. Phys.*, **20**, 261-268, (1987).

[16] G. Horvay, R. Mani, M. A. Veluswami and G. E. Zinsmeister, "Transient Heat Conduction in Laminated Composites", *J. Heat Trans.*, **95**, 309-316, (1973).

[17] L. S. Han and A. A. Cosner, "Effective Thermal Conductivities of Fibrous Composites", *J. Heat Trans.*, **103**, 387-392, (1981).

[18] Y. Benveniste and T. Miloh, "The Effective Conductivity of Composites with Imperfect Thermal Contact at Constituent Interfaces", *Int. J. Engng. Sci.*, **24**, 1537-1552, (1986).

[19] D. P. H. Hasselman and L. F. Johnson, "Effective Thermal Conductivity of Composites with Interfacial Thermal Barrier Resistance", *J. Comp. Mat.*, **21**, 508-515, (1987).

[20] D. P. H. Hasselman, "Thermal Diffusivity and Conductivity of Composites with Interfacial Thermal Contact Resistance", *Thermal Conductivity*, **20**, 405-413, (1987).

[21] D. P. H. Hasselman, A. Venkateswaran and H. Tawil, "Role of Interfacial Debonding and Matrix Cracking in the Effective Diffusivity of Alumina-Fiber-Reinforced Chemical-Vapor-Infiltrated Silicon Carbide Matrix Composites", *J. Am. Ceram. Soc.*, **74**, 1631-1634, (1991).

[22] W. J. Parker, R. J. Jenkins, C. P. Butler and G. L. Abbott, "Flash Method of Determining Thermal Diffusivity, Heat Capacity, and Thermal Conductivity", *J. Appl. Phys.*, **32**, 1679-1684, (1961).

[23] R. E. Taylor, "Heat-pulse Thermal Diffusivity Measurements", *High Temp.-High Pressures*, **11**, 43-58, (1979).

[24] R. E. Taylor, J. Jortner and H. Groot, "Thermal Diffusivity of Fiber-Reinforced Composites Using the Laser Flash Technique", *Carbon*, **23**, 215-222, (1985).

[25] D. L. Balageas and A. M. Luc, "Transient Thermal Behavior of Directional Reinforced Composites: Applicability Limits of Homogeneous Property Models", *AIAA J.*, **24**, 109-114, (1986).

[26] D. P. H. Hasselman, K. Y. Donaldson, H. D. Bhatt, J. R. Thomas, Jr., C. M. Alvarado, E. P. Hurst, II, "Thermal Conductivity/Diffusivity of a Carbon Fiber-Reinforced Glass Matrix Composite with Partial Fiber-Matrix Thermal Contact", to be presented at the 22nd International Thermal Conductivity Conference, (1993).

[27] M. N. Ozisik, *Heat Conduction*, pp 595-596, Wiley, New York (1980).

[28] ibid, p 300.

[29] ibid, p 33.

[30] ibid, pp 608-610.

[31] ibid, p 598.

[32] ibid, ch 5.

[33] ibid, p 196.

[34] R. E. Taylor and L. M. Clark, III, "Finite Pulse Time Effects in Flash Diffusivity Method", *High Temp.-High Pressures*, **6**, 65-72, (1974).

APPENDIX

```
C23456789 123456789 123456789 123456789 123456789 123456789 123456789 12
      IMPLICIT DOUBLE PRECISION (A-H,O-Z)
      DOUBLE PRECISION T(500,10),TO(500,10),R(10), RN(10), RTX(10),
     $              RTR(10), RST(10), AR(10), X(500)

C-----------------------------------------------------------------------
C  Computer program to calcualte the temperature distribution in a
C  fiber-reinforced composite using an arbitrary number of axial and
C  radial nodes
C
C  Y is the axial length of the composite
C  RI is the radius of the fiber
C  RO is the outer radius of the matrix
C  AK1 is the thermal conductivity of the fiber
C  AK2 is the thermal conductivity of the matrix
C  CP1 is the heat capacity of the fiber
C  CP2 is the heat capacity of the matrix
C  RHO1 is the density of the fiber
C  RHO2 is the density of the matrix
C  Q is the energy flux coming from the laser
C  H is the natural convection coefficient
C  HC is the contact conductance
C  DELT is the time step for calculations
C  PULSE is the duration of the energy pulse
C  NNR1 is the number of nodes radial in the fiber
C  NNR2 is the number of radial nodes in the matrix
C  NNX is the number of axial nodes
C  DELX is the axial dimension of the control volumes
C  DELR1 is the radial dimension of the control volumes in the fiber
C  DELR2 is the radial dimension of the control volumes in the matrix
C  R(j) is the radial control volume face location of node i,j
C  X(i) is the axial location of node i,j
C  RN(j) is the radial node location of node i,j
C  AR(j) is the axial area of control volume i,j
C  RTX(j) is the resistance to heat transfer between nodes in row j
C  RTR(j) is the resistance to heat transfer between radial nodes j&j-1
C  T(i,j) is the new temperature for node i,j
C  TO(i,j) is the old temperature for node i,j
C-----------------------------------------------------------------------
      INTEGER STEP
```

```
      OPEN (1, FILE='output')
      Y = 1.D-3
      RI = 5.D-6
      RO = DSQRT(2.D0)*RI
      AK1 = 1.D2
      AK2 = 1.D0
      CP1 = 717.D0
      CP2 = 766.D0
      RHO1 = 2000.D0
      RHO2 = 2160.D0
      HC1 = RHO1*CP1
      HC2 = RHO2*CP2
      Q = 10.D6
      H = 5.D0
      HC = 1.D4
      DELT  = 1.D-4
      PULSE = 1.D-3
      NNR1 = 3
      NNR2 = 3
      NNX  = 400
      STEP = NNX/10
      NRT = NNR1 + NNR2
      DELX = Y/DBLE(NNX-1)
      DELR1 = RI/( DBLE(NNR1)-.5D0 )
      DELR2 = (RO-RI)/( DBLE(NNR2)-.5D0 )
C-------------------------------------------------------------------------
C23456789 123456789 123456789 123456789 123456789 123456789 123456789 12
C  Radial control volume face location
      R(1) = DELR1/2.D0
      DO 5 JR1 = 2, NNR1
         R(JR1) =  R(1) + DBLE(JR1-1)*DELR1
  5   CONTINUE

      DO 10 JR2 = 1, NNR2-1
         R(NNR1+JR2) = R(NNR1) + DBLE(JR2)*DELR2
 10   CONTINUE
      R(NRT) = RO
C-------------------------------------------------------------------------
C23456789 123456789 123456789 123456789 123456789 123456789 123456789 12
C  Node location in the axial and radial directions

      DO 15 I = 2, NNX
         X(I) = DELX*DBLE(I-1)
 15   CONTINUE

      DO 20 JN1 = 2, NNR1
         RN(JN1) = DBLE(JN1-1)*DELR1
 20   CONTINUE

      RN(NNR1+1) = RI + DELR2/2.D0
      DO 25 JN2 = 2, NNR2
         RN(NNR1+JN2) = RN(NNR1+1) + DBLE(JN2-1)*DELR2
 25   CONTINUE
C-------------------------------------------------------------------------
C23456789 123456789 123456789 123456789 123456789 123456789 123456789 12
C  Areas and thermal resistances

      AR(1) = (DELR1/2.D0)**2
      DO 30 JA1 = 2, NNR1
         AR(JA1) = ( R(JA1)+R(JA1-1) )*DELR1
 30   CONTINUE

      DO 35 JA2 = 1, NNR2-1
         AR(NNR1+JA2) = ( R(NNR1+JA2)+R(NNR1+JA2-1) )*DELR2
 35   CONTINUE
```

```
      AR(NRT) = ( RO+R(NRT-1) )*DELR2/2.D0

      DO 40 JR1 = 2, NNR1
         RTX(JR1) = DELX/AK1/AR(JR1)
         RST(JR1) = HC1*AR(JR1)*DELX/DELT
 40   CONTINUE

      DO 45 JR2 = 1, NNR2
         RTX(NNR1+JR2) = DELX/AK2/AR(NNR1+JR2)
         RST(NNR1+JR2) = HC2*AR(NNR1+JR2)*DELX/DELT
 45   CONTINUE

      RTR(1) = 1.D20
      DO 50 JR3 = 2, NNR1-1
         RTR(JR3) = DLOG( RN(JR3+1)/RN(JR3) )/DELX/AK1/2.D0
 50   CONTINUE
      RINT = ( DLOG( RI/RN(NNR1) )/DELX/AK1 + 1.D0/HC/RI/DELX +
     $          DLOG(RN(NNR1+1)/RI)/DELX/AK2 )/2.D0
      DO 55 JR4 = 1, NNR2-1
         RTR(NNR1+JR4) = DLOG( RN(NNR1+JR4+1)/RN(NNR1+JR4) )/
     $                   DELX/AK2/2.D0
 55   CONTINUE
C-----------------------------------------------------------------------
C23456789 123456789 123456789 123456789 123456789 123456789 123456789 12
C   Finite difference equations
C
C                                 Last Row
 60   KNTER = 1 + KNTER
      RC = 1.D0/H/AR(NRT)
      T(NNX,NRT)=( Q*AR(NRT) + T(NNX,NRT-1)/RTR(NRT-1)/2.D0 +
     $T(NNX-1,NRT)/RTX(NRT) + TO(NNX,NRT)*RST(NRT)/2.D0 )/
     $( .5D0/RTR(NRT-1) + 1.D0/RTX(NRT) + 1.D0/RC + RST(NRT)/2.D0 )

      T(1,NRT) = ( T(1,NRT-1)/RTR(NRT-1)/2.D0 +
     $T(2,NRT)/RTX(NRT) + TO(1,NRT)*RST(NRT)/2.D0 )/( .5D0/RTR(NRT-1) +
     $1.D0/RTX(NRT) + RST(NRT)/2.D0 )

      DO 100 I = 2, NNX-1
      T(I,NRT) = ( (T(I-1,NRT)+T(I+1,NRT))/RTX(NRT) +
     $T(I,NRT-1)/RTR(NRT-1) + TO(I,NRT)*RST(NRT) )/( 2.D0/RTX(NRT) +
     $1.D0/RTR(NRT-1) + RST(NRT) )
 100  CONTINUE
C-----------------------------------------------------------------------
C23456789 123456789 123456789 123456789 123456789 123456789 123456789 12
C                              Fiber section
      DO 200 J = 2, NNR1-1
         DO 250 I = 2, NNX-1
         T(I,J) = ( (T(I-1,J)+T(I+1,J))/RTX(J) +
     $   T(I,J-1)/RTR(J-1) + T(I,J+1)/RTR(J) + TO(I,J)*RST(J) )/
     $   ( 2.D0/RTX(J) + 1.D0/RTR(J-1) + 1.D0/RTR(J) + RST(J) )
 250     CONTINUE
 200  CONTINUE

C                              Matrix section
      DO 300 J = NNR1+2, NRT-1
         DO 350 I = 2, NNX-1
         T(I,J) = ( (T(I-1,J)+T(I+1,J))/RTX(J) +
     $   T(I,J-1)/RTR(J-1) + T(I,J+1)/RTR(J) + TO(I,J)*RST(J) )/
     $   ( 2.D0/RTX(J) + 1.D0/RTR(J-1) + 1.D0/RTR(J) + RST(J) )
 350     CONTINUE
 300  CONTINUE
C-----------------------------------------------------------------------
C23456789 123456789 123456789 123456789 123456789 123456789 123456789 12
C                           Fiber at the interface
      RC = 1.D0/H/AR(NNR1)
```

```
      T(NNX,NNR1) = ( Q*AR(NNR1) + T(NNX,NNR1+1)/RINT/2.D0 +
     $T(NNX-1,NNR1)/RTX(NNR1) + T(NNX,NNR1-1)/RTR(NNR1-1)/2.D0 +
     $TO(NNX,NNR1)*RST(NNR1)/2.D0 )/
     $( .5/RINT + 1.D0/RTX(NNR1) + .5D0/RTR(NNR1-1) + 1.D0/RC +
     $ RST(NNR1)/2.D0 )

      T(1,NNR1) = ( T(1,NNR1+1)/RINT/2.D0 + T(2,NNR1)/RTX(NNR1) +
     $T(1,NNR1-1)/RTR(NNR1-1)/2.D0 + TO(1,NNR1)*RST(NNR1)/2.D0 )/
     $( .5D0/RINT + 1.D0/RTX(NNR1) + .5D0/RTR(NNR1-1) +RST(NNR1)/2.D0)

      DO 400 I = 2, NNX-1
      T(I,NNR1) = ( (T(I-1,NNR1)+T(I+1,NNR1))/RTX(NNR1) +
     $T(I,NNR1+1)/RINT + T(I,NNR1-1)/RTR(NNR1-1) + TO(I,NNR1)*RST(NNR1))
     $/( 2.D0/RTX(NNR1) + 1.D0/RINT + 1.D0/RTR(NNR1-1) + RST(NNR1) )
 400  CONTINUE
C-----------------------------------------------------------------------
C23456789 123456789 123456789 123456789 123456789 123456789 123456789 12
C                          Matrix at the interface
      RC = 1.D0/H/AR(NNR1+1)
      T(NNX,NNR1+1)=(Q*AR(NNR1+1) + T(NNX,NNR1)/RINT/2.D0 +
     $T(NNX-1,NNR1+1)/RTX(NNR1+1) + T(NNX,NNR1+2)/RTR(NNR1+1)/2.D0 +
     $TO(NNX,NNR1+1)*RST(NNR1+1)/2.D0 )/( 1.D0/RC +.5D0/RINT +
     $1.D0/RTX(NNR1+1) + .5D0/RTR(NNR1+1) + RST(NNR1+1)/2.D0 )

      T(1,NNR1+1) = ( T(1,NNR1)/RINT/2.D0 + T(2,NNR1+1)/RTX(NNR1+1) +
     $T(1,NNR1+2)/RTR(NNR1+1)/2.D0 + TO(1,NNR1+1)*RST(NNR1+1)/2.D0 )/
     $( .5D0/RINT + 1.D0/RTX(NNR1+1) +.5D0/RTR(NNR1+1)+RST(NNR1+1)/2.D0)

      DO 450 I = 2, NNX-1
      T(I,NNR1+1) = ( (T(I-1,NNR1+1)+T(I+1,NNR1+1))/RTX(NNR1+1) +
     $T(I,NNR1)/RINT+T(I,NNR1+2)/RTR(NNR1+1) + TO(I,NNR1+1)*RST(NNR1+1))
     $/( 2.D0/RTX(NNR1+1) + 1.D0/RINT + 1.D0/RTR(NNR1+1) + RST(NNR1+1) )
 450  CONTINUE
C-----------------------------------------------------------------------
C23456789 123456789 123456789 123456789 123456789 123456789 123456789 12

      DO 500 J = 2, NNR1-1
      RC = 1.D0/H/AR(J)
      T(NNX,J)=(Q*AR(J) + T(NNX,J+1)/RTR(J)/2.D0 + T(NNX-1,J)/RTX(J) +
     $T(NNX,J-1)/RTR(J-1)/2.D0 + TO(NNX,J)*RST(J)/2.D0 )/( .5D0/RTR(J)+
     $1.D0/RTX(J) + .5D0/RTR(J-1) + 1.D0/RC + RST(J)/2.D0 )
      T(1,J) = ( T(1,J+1)/RTR(J)/2.D0 + T(2,J)/RTX(J) +
     $T(1,J-1)/RTR(J-1)/2.D0 + TO(1,J)*RST(J)/2.D0 )/( .5D0/RTR(J) +
     $1.D0/RTX(J) + .5/RTR(J-1) + RST(J)/2.D0 )
 500  CONTINUE

      DO 550 J = NNR1+2, NRT-1
      RC = 1.D0/H/AR(J)
      T(NNX,J)=(Q*AR(J) + T(NNX,J+1)/RTR(J)/2.D0 + T(NNX-1,J)/RTX(J) +
     $T(NNX,J-1)/RTR(J-1)/2.D0 + TO(NNX,J)*RST(J)/2.D0 )/( .5D0/RTR(J) +
     $1.D0/RTX(J) + .5D0/RTR(J-1) + 1.D0/RC + RST(J)/2.D0 )
      T(1,J) = ( T(1,J+1)/RTR(J)/2.D0 + T(2,J)/RTX(J) +
     $T(1,J-1)/RTR(J-1)/2.D0 + TO(1,J)*RST(J)/2.D0 )/( .5/RTR(J) +
     $1.D0/RTX(J) + .5/RTR(J-1) + RST(J)/2.D0 )
 550  CONTINUE

      DO 600 I = 1, NNX
         T(I,1) = T(I,2)
 600  CONTINUE
      KNTER = KNTER + 1
C-----------------------------------------------------------------------
C23456789 123456789 123456789 123456789 123456789 123456789 123456789 12
      IF (KNTER .EQ. 250) THEN
      EPS = ABS( T(NNX,2) - TEST )/T(NNX,2)
      TEST = T(NNX,2)
```

```
      WRITE (*,*) T(NNX,2)
      KNTER = 0
      IF (EPS .LT. 1.D-4) THEN
              DO 601 J = 1, NRT
               EOUT = EOUT + AR(J)*H*T(NNX,J)*DELT
               TAVG = TAVG + T(1,J)
601           CONTINUE

              DO 602 I = 2, NNX-1
              DO 603 J = 1, NNR1
                EST1 = EST1 + AR(J)*DELX*HC1*T(I,J)
603           CONTINUE
              DO 604 J = NNR1+1, NRT
                EST2 = EST2 + AR(J)*DELX*HC2*T(I,J)
604           CONTINUE
602           CONTINUE

              DO 605 J = 1, NNR1
               EST1 = EST1 + AR(J)*DELX/2.D0*HC1*(T(1,J)+T(NNX,J))
605           CONTINUE
              DO 606 J = NNR1+1, NRT
               EST2 = EST2 + AR(J)*DELX/2.D0*HC2*(T(1,J)+T(NNX,J))
606           CONTINUE

              EIN = EIN + Q*RO**2*DELT
             KKNTER = KKNTER + 1
             WRITE (1,902) DELT*REAL(KKNTER), NNX
              WRITE (*,902) DELT*REAL(KKNTER), NNX
 901         WRITE (1,*) 'x (mm) ='
             WRITE (*,*) 'x (mm) ='
 902         FORMAT ('Temperature for time t = ',D10.4,'s.  NNX=',I4)
             WRITE (1,905) (X(I)*1.D3, I = 1, NNX, STEP)
             WRITE (*,905) (X(I)*1.D3, I = 1, NNX, STEP)
             WRITE (1,*)
             WRITE (*,*)
             DO 910 J = NRT, 1, -1
             WRITE (*,905) (T(I,J), I = 1, NNX, STEP)
             WRITE (1,905) (T(I,J), I = 1, NNX, STEP)
 905         FORMAT (10F7.2)
 910         CONTINUE
             TIME = DELT*DBLE(KKNTER)
             WRITE (1,*)
              IF (DELT*REAL(KKNTER) .GE. PULSE) THEN
            Q = 0.D0
              END IF
              DO 915 I = 1, NNX
              DO 915 J = 1, NRT
                 TO(I,J) = T(I,J)
 915          CONTINUE
              EST1 = 0.D0
              EST2 = 0.D0
              TAVG = 0.D0
      END IF
      END IF

      GOTO 60
 999  STOP
      END
```

```
C23456789 123456789 123456789 123456789 123456789 123456789 123456789 12
      IMPLICIT DOUBLE PRECISION (A-H,O-Z)
      DOUBLE PRECISION BETA(5000), NU(5000)
      DOUBLE PRECISION XNORM1(5000), XNORM2(5000), X(20), NX
      DOUBLE PRECISION TT1(100), TT2(100)

C-----------------------------------------------------------------------
C  Computer program to calcualte the exact temperature distribution in a
C  fiber-reinforced composite
C
c  Y is the axial length of the composite
C  RI is the radius of the fiber
C  RO is the outer radius of the matrix
C  AK1 is the thermal conductivity of the fiber
C  AK2 is the thermal conductivity of the matrix
C  CP1 is the heat capacity of the fiber
C  CP2 is the heat capacity of the matrix
C  RHO1 is the density of the fiber
C  RHO2 is the density of the matrix
C  Q is the energy flux coming from the laser
C  H is the natural convection coefficient
C  HC is the contact conductance
C  DELT is the time step for calculations
C  TAU is the duration of the energy pulse
C  NNX is the number of axial nodes
C  DELX is the axial dimension of the control volumes
C  DELR1 is the radial dimension of the control volumes in the fiber
C  DELR2 is the radial dimension of the control volumes in the matrix
C  X(i) is the axial location of node i,j
C  BETA(i) are the eigenvalues for the fiber
C  NU(i) are the eigenvalues for the matrix]
C  XNORM1(i) are the nomalization integrals in the fiber
C  XNORM2(i) are the nomalization integrals in the matrix
C  T(i,j) is the new temperature for node i,j
C-----------------------------------------------------------------------

      OPEN (1, FILE='temp')
      Y = 2.D-3
      AK1 = 1.D2
      AK2 = 1.D0
      CP1 = 717.D0
      CP2 = 766.D0
      RHO1 = 2000.D0
      RHO2 = 2160.D0
      ALPHA1 = AK1/CP1/RHO1
      ALPHA2 = AK2/CP2/RHO2
      Q =  20.D6
      H = 5.D-20
      TAU = .5D-3
      DELT = 12.5D-3
      NNX = 2
      DELX = Y/DBLE(NNX)
      X(1) = .000D0
      X(2) = Y

      H1 = H/AK1
      H2 = H/AK2

      EFX1O = -1.D0
      EFX2O = -1.D0
      BX = 0.D0
      NX = 0.D0
      KK = 0
      JX1 = 0
      MM = 0
```

```
      JX2 = 0
C-----------------------------------------------------------------------
C Calculate eigenvalues in the x direction
  9   STEPB = 1.D-1
 10   BX = BX + STEPB

      EFX1 = BX*DSIN(BX*Y)-H1*DCOS(BX*Y)

      RATIO = EFX1/EFX1O
      IF (RATIO .LT. 0.D0) THEN

      IF (KK .EQ. 9) THEN
      EFX1O = EFX1
      KK = 0
      JX1 = JX1 + 1
      BETA(JX1) = BX
      XNORM1(JX1) = (Y*(BX**2+H1**2)+H1)/(BX**2+H1**2)/2.D0
      STEPB = 1.D0
      GOTO 25
      END IF

      BX = BX - STEPB
      STEPB = STEPB/10.D0
      KK = KK + 1
      GOTO 10
      END IF

      EFX1O = EFX1
      GOTO 10

 25   IF (JX1 .EQ. 300) THEN
      GOTO 29
      END IF
      GOTO 10
C-----------------------------------------------------------------------
C Calculate eigenvalues in the x direction
 29   STEPN = 1.D-1
 30   NX = NX + STEPN

      EFX2 = NX*DSIN(NX*Y)-H2*DCOS(NX*Y)

     RATIO = EFX2/EFX2O
      IF (RATIO .LT. 0.D0) THEN

      IF (MM .EQ. 9) THEN
      EFX2O = EFX2
      MM = 0
      JX2 = JX2 + 1
      NU(JX2) = NX
      XNORM2(JX2) = (Y*(NX**2+H2**2)+H2)/(NX**2+H2**2)/2.D0
      STEPN = 1.D0
      GOTO 60
      END IF

      NX = NX - STEPN
      STEPN = STEPN/10.D0
      MM = MM + 1
      GOTO 30
      END IF

      EFX2O = EFX2
      GOTO 30

  60  IF (JX2 .EQ. 3000) THEN
      GOTO 70
```

```
      END IF

      GOTO 30
C-----------------------------------------------------------------------
C   Calculation of temperature distribution in region 1
  70  KNTER = KNTER + 1
      TIME = DBLE(KNTER)*DELT
      DO 220 MX = 1, NNX
         DO 240 KX1 = 1, JX1
            X1 = DCOS(BETA(KX1)*X(MX))

            IF (TIME .LE. TAU) THEN
          T1 = X1/XNORM1(KX1)*DCOS(BETA(KX1)*Y)/BETA(KX1)**2*
     $              (1.D0 - DEXP(-ALPHA1*BETA(KX1)**2* TIME) )
              GOTO 230
            END IF

            T1 = X1/XNORM1(KX1)*DCOS(BETA(KX1)*Y)/BETA(KX1)**2*
     $           ( DEXP(-ALPHA1*BETA(KX1)**2*(TIME-TAU)) -
     $             DEXP(-ALPHA1*BETA(KX1)**2* TIME) )
 230        T1S = T1S + Q/AK1*T1
 240        CONTINUE
      TT1(MX) = T1S
      T1S = 0.D0
 220  CONTINUE
C-----------------------------------------------------------------------
C   Calculation of temperature distribution in region 2
      DO 320 MX = 1, NNX
         DO 340 KX2 = 1, JX2
            X2 = DCOS(NU(KX2)*X(MX))
            IF (TIME .LE. TAU) THEN
               T2 = X2/XNORM2(KX2)*DCOS(NU(KX2)*Y)/NU(KX2)**2*
     $              (1.D0 - DEXP(-ALPHA2*NU(KX2)**2* TIME) )
              GOTO 330
            END IF
            T2 = X2/XNORM2(KX2)*DCOS(NU(KX2)*Y)/NU(KX2)**2*
     $           ( DEXP(-ALPHA2*NU(KX2)**2*(TIME-TAU)) -
     $             DEXP(-ALPHA2*NU(KX2)**2* TIME) )
 330        T2S = T2S + Q/AK2*T2
 340        CONTINUE
      TT2(MX) = T2S
      T2S = 0.D0
 320  CONTINUE

      WRITE (1,902) DELT*DBLE(KNTER)
      WRITE (*,902) DELT*DBLE(KNTER)
 902  FORMAT ('Temperature for time t = ',D10.4,'s.')
      WRITE(1,*) 'x (mm) ='
      WRITE(*,*) 'x (mm) ='
      WRITE (1,905) (X(I)*1.D3, I = 1, 10)
      WRITE (*,905) (X(I)*1.D3, I = 1, 10)
      WRITE (1,*)
      WRITE (*,*)
      WRITE (1,905) (TT2(I), I = 1, 10)
      WRITE (*,905) (TT2(I), I = 1, 10)
      WRITE (1,905) (TT1(I), I = 1, 10)
      WRITE (*,905) (TT1(I), I = 1, 10)
 905  FORMAT (10F7.2)
 910  GOTO 70
      STOP
    END
```